VASP: beyond DFT
The Random Phase Approximation

University of Vienna,
Faculty of Physics and Center for Computational Materials Science,
Vienna, Austria

PAST, PRESENT, FUTURE

- PAST

  - The Workhorse: DFT

  - Efficient and stable algorithms

  - PAW datasets

- PRESENT

  - Beyond DFT, and beyond the groundstate:
    Hybrid functionals, linear response, RPA (GW & ACFTD), BSE

- FUTURE

  - Near future: cubic-scaling-RPA

  - …

Need to go beyond DFT and Hartree-Fock?

Lattice constants and Bulk moduli:
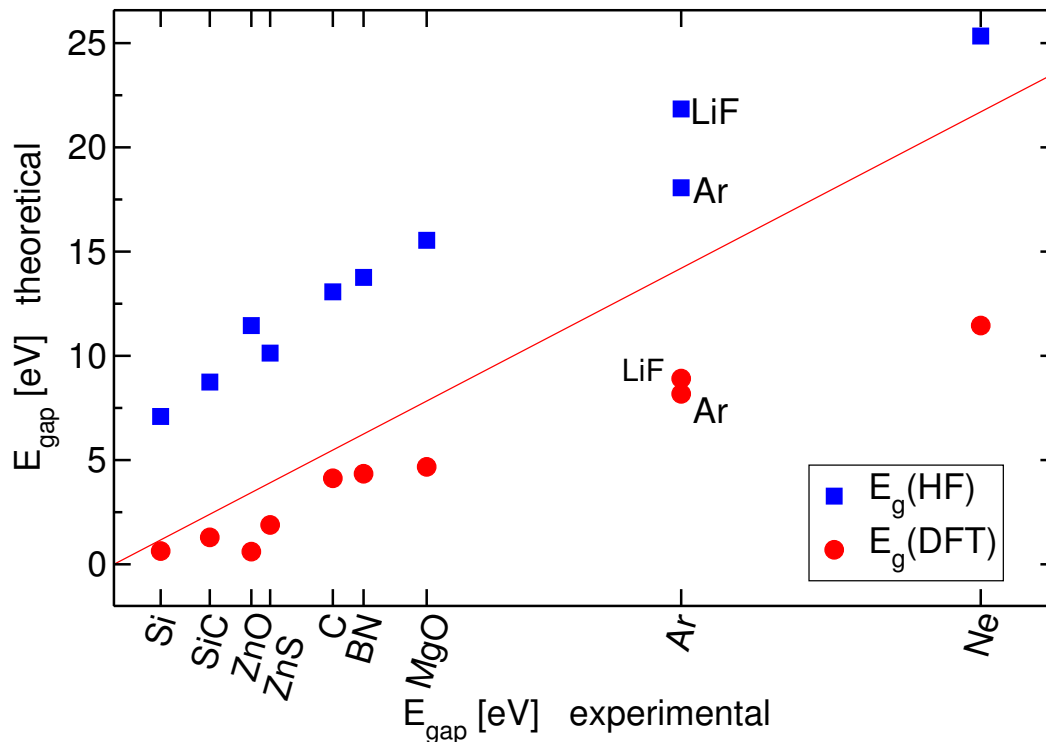AlP, AlAs, BAs, BP, Si, C, SiC, MgO, LiF

	LDA Δa_0	LDA ΔB_0	PBE Δa_0	PBE ΔB_0	HF Δa_0	HF ΔB_0
MRE	-1.4	3.5	0.8	-7.2	0.4	8.2
MARE	1.4	7.9	0.8	7.2	0.7	8.2

(All in %)

Atomization energy

	LDA	PBE
MRE (%)	17.3	-1.9
MARE (%)	17.3	3.4
ME (eV)	0.76	0.14

Band gaps

(More) accurate treatment of electronic correlation needed for, e.g:

- Band gaps (optical properties
- Total energy differences with chemical accuracy (1 kcal/mol ≈ 40 meV)
- Atomization and formation energies
- Reaction barriers
- Van der Waals interactions

Catalysis: dehydrogenation of propane in Mordenite

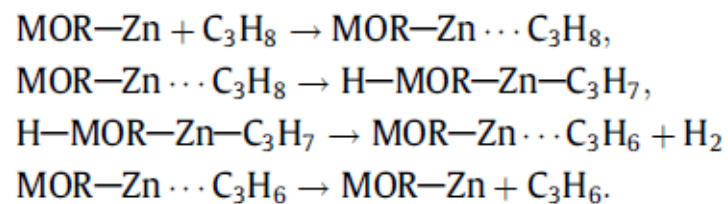$$MOR-Zn + C_3H_8 \rightarrow MOR-Zn \cdots C_3H_8,$$
$$MOR-Zn \cdots C_3H_8 \rightarrow H-MOR-Zn-C_3H_7,$$
$$H-MOR-Zn-C_3H_7 \rightarrow MOR-Zn \cdots C_3H_6 + H_2$$
$$MOR-Zn \cdots C_3H_6 \rightarrow MOR-Zn + C_3H_6.$$
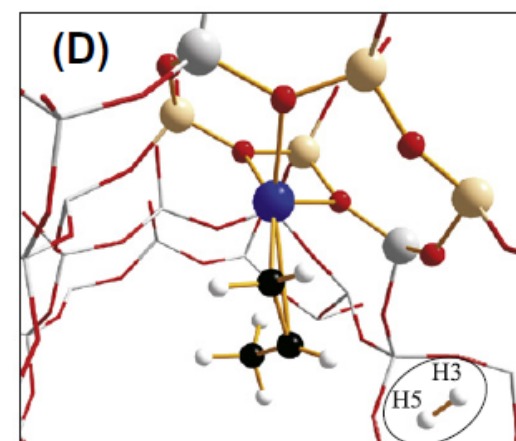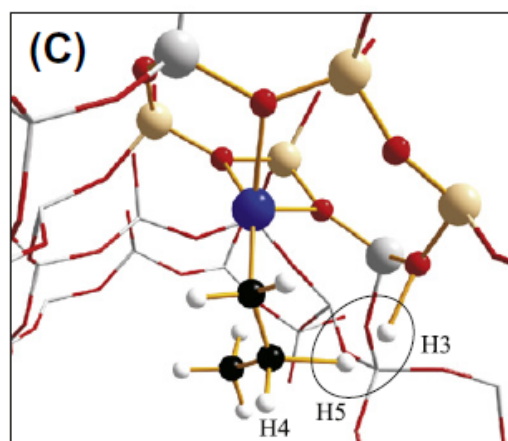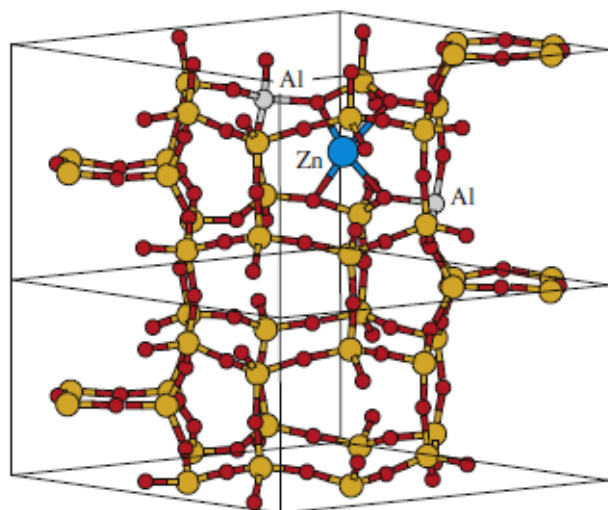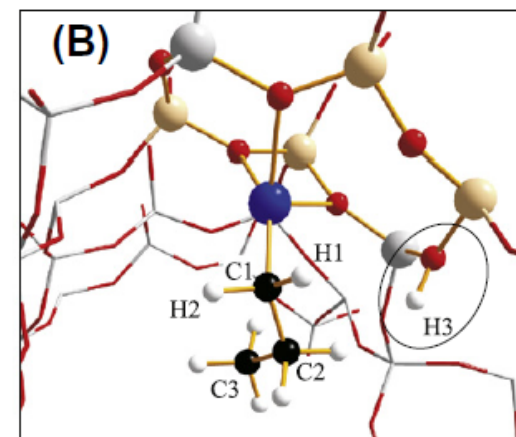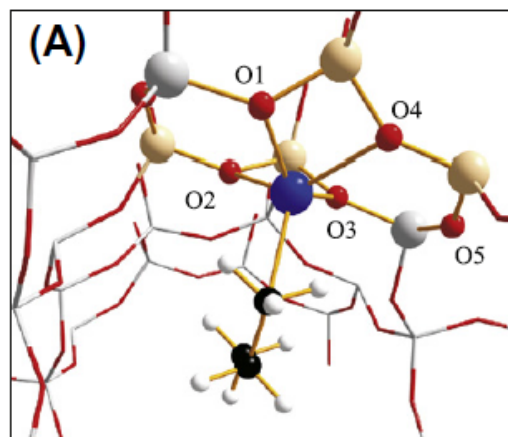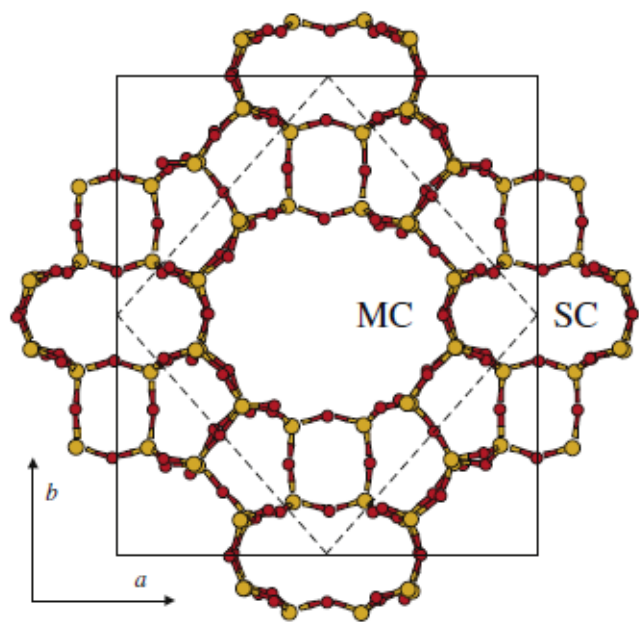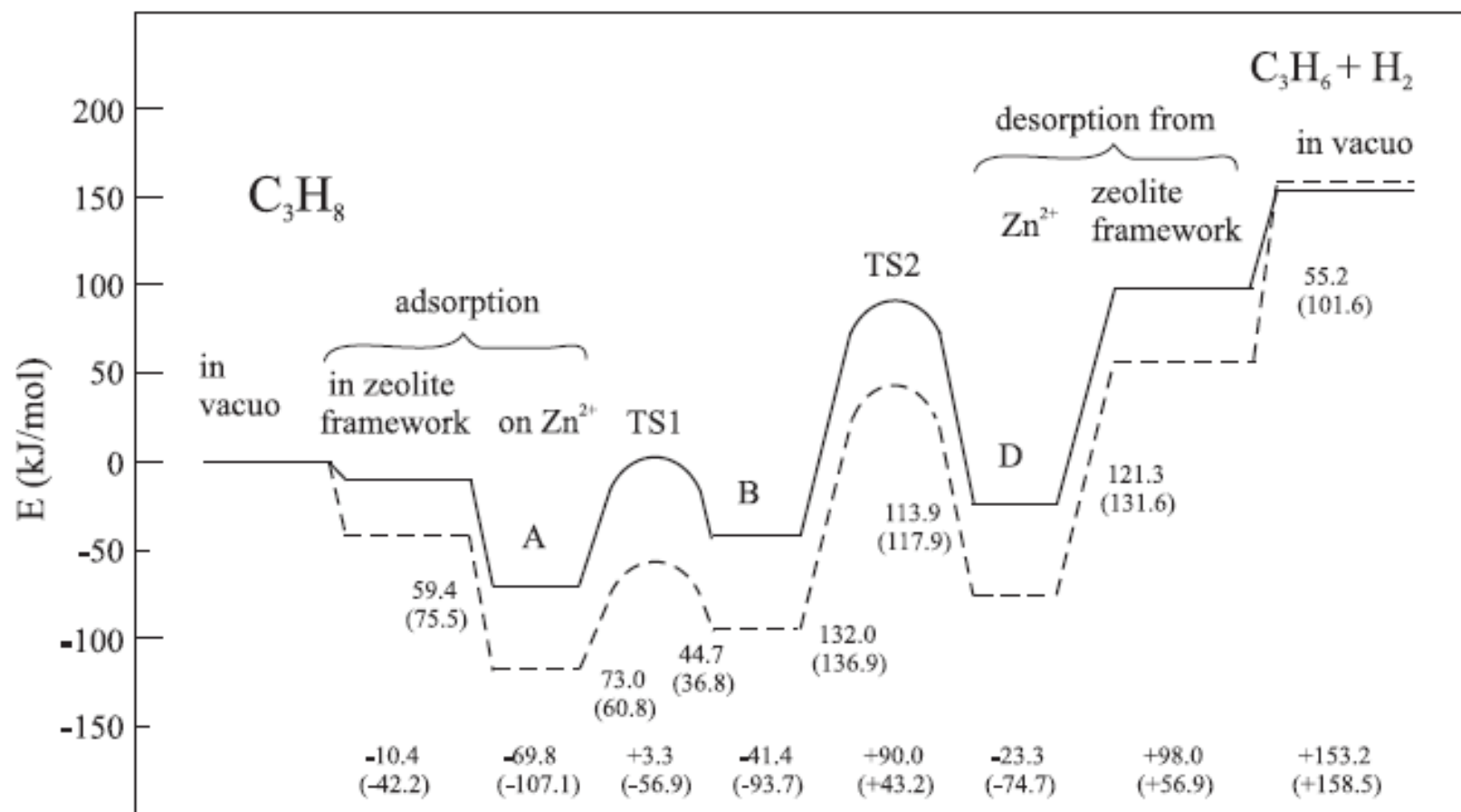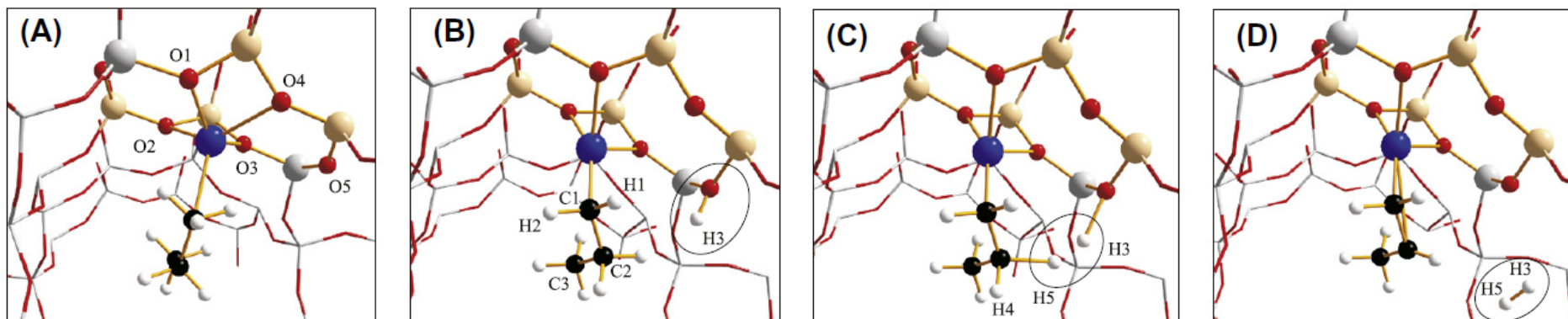
New density functionals (for solids)

AM05

Functional designed to include surface effects in self-consistent density functional theory

R. Armiento[1,*] and A. E. Mattsson[2,†]

[1]*Department of Physics, Royal Institute of Technology, AlbaNova University Center, SE-106 91 Stockholm, Sweden*
[2]*Computational Materials and Molecular Biology MS 1110, Sandia National Laboratories, Albuquerque,
New Mexico 87185-1110, USA*

PBEsol

Restoring the Density-Gradient Expansion for Exchange in Solids and Surfaces

John P. Perdew,[1] Adrienn Ruzsinszky,[1] Gábor I. Csonka,[2] Oleg A. Vydrov,[3] Gustavo E. Scuseria,[3] Lucian A. Constantin,[4]
Xiaolan Zhou,[1] and Kieron Burke[5]

[1]*Department of Physics and Quantum Theory Group, Tulane University, New Orleans, Louisiana 70118, USA*
[2]*Department of Chemistry, Budapest University of Technology and Economics, H-1521 Budapest, Hungary*
[3]*Department of Chemistry, Rice University, Houston, Texas 77005, USA*
[4]*Donostia International Physics Center, E-20018, Donostia, Basque Country*
[5]*Departments of Chemistry and of Physics, University of California, Irvine, Irvine, California 92697, USA*

AM05 & PBEsol

TABLE I. Statistical data for the equilibrium lattice constants (Å) of the 18 test solids of Ref. 38 at 0 K calculated from the SJEOS. The Murnaghan EOS yields identical results within the reported number of decimal places. Experimental low temperature (5–50 K) lattice constants are from Ref. 56 (Li), Ref. 57 (Na, K), Ref. 58 (Al, Cu, Rh, Pd, Ag), and Ref. 59 (NaCl). The rest are based on room temperature values from Ref. 60 (C, Si, SiC, Ge, GaAs, NaF, LiF, MgO) and Ref. 57 (LiCl), corrected to the $T=0$ limit using the thermal expansion from Ref. 58. An estimate of the zero-point anharmonic expansion has been subtracted out from the experimental values (cf. Table II). (The calculated values are precise to within 0.001 Å for the given basis sets, although GAUSSIAN GTO1 and GTO2 basis-set incompleteness limits the accuracy to 0.02 Å.) GTO1: the basis set used in Ref. 38. GTO2: For C, Si, SiC, Ge, GaAs, and MgO, the basis sets were taken from Ref. 41. For the rest of the solids, the GTO1 basis sets and effective core potentials from Ref. 38 were used. The best theoretical values are in boldface. The LDA, PBEsol, and PBE GTO2 results are from Ref. 14. The SOGGA GTO1 results are from Ref. 15.

	LDA	LDA	PBEsol	PBEsol	PBEsol	AM05	SOGGA	PBE	PBE	PBE	TPSS
	GTO2	VASP	GTO2	BAND	VASP	VASP	GTO1	GTO2	VASP	BAND	BAND
ME[a] (Å)	−0.047	−0.055	0.022	**0.010**	**0.012**	0.029	**0.009**	0.075	0.066	0.063	0.048
MAE[b] (Å)	0.050	0.050	0.030	**0.023**	**0.023**	0.036	**0.024**	0.076	0.069	0.067	0.052
MRE[c] (%)	−1.07	−1.29	0.45	**0.19**	**0.24**	0.58	**0.19**	1.62	1.42	1.35	0.99
MARE[d] (%)	1.10	1.15	0.67	**0.52**	**0.52**	0.80	**0.50**	1.65	1.48	1.45	1.10

Meta-GGAs

Lattice constant

	MRE	MARE
LDA	-1.73	1.73
PBE	1.10	1.29
PBEsol	-0.24	0.73
AM05	0.19	0.75
TPSS	0.73	0.90
revTPSS	0.29	0.68

Atomization energy (solids)

	MRE	MARE
LDA	16.5	16.5
PBE	-3.68	4.23
PBEsol	5.97	6.52
TPSS	-1.99	4.70
revTPSS	1.22	5.73

Atomization energy (AE6 mol.)

	MRE	MARE
PBE	3.2	4.2
PBEsol	8.1	8.1
TPSS	1.3	2.4
revTPSS	1.3	2.8

$$E_{\mathrm{xc}} = \int d\mathbf{r}\, n\epsilon_{\mathrm{xc}}(n, \nabla n, \tau) \qquad \tau = \sum_i 1/2 |\nabla \psi_i|^2$$
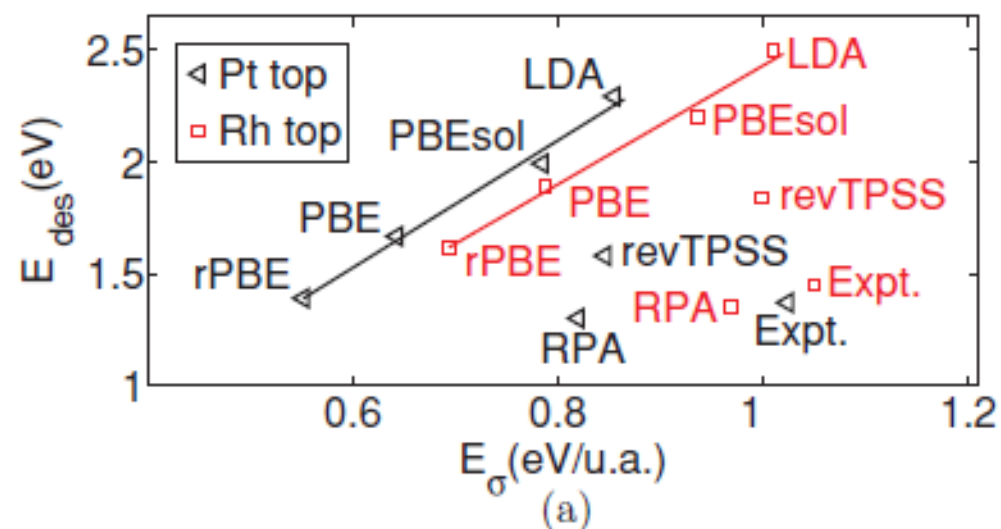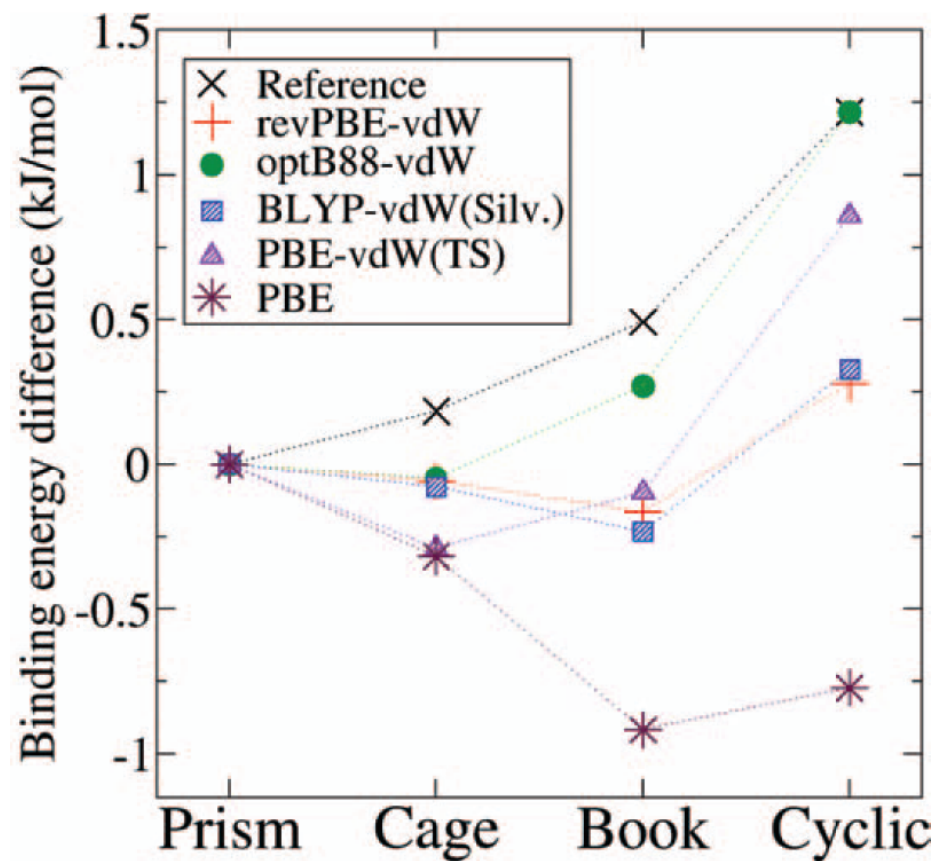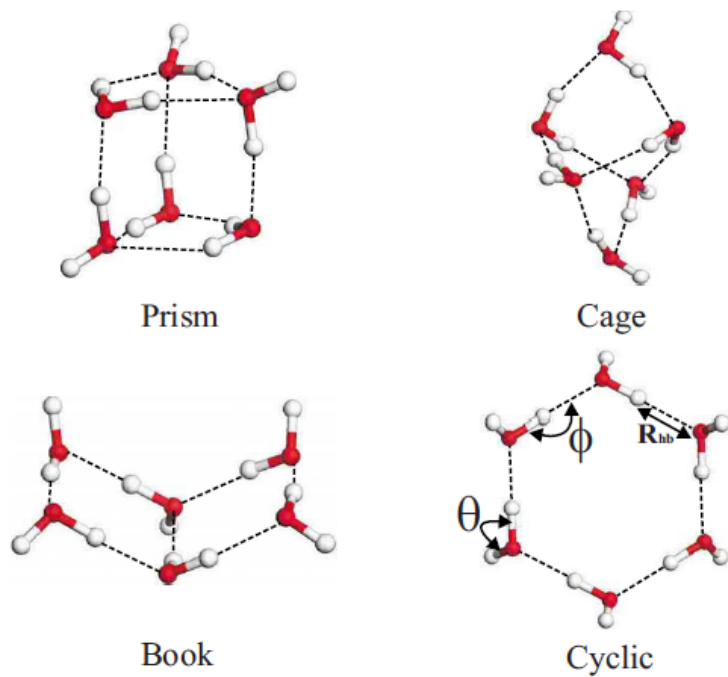

FIG. 1. (Color) (a) Atop CO desorption energy vs surface energies for Pt(111) and Rh(111). RPA values from Ref. 5, experimental surface energies from liquid-metal data (Refs. 23 and 24), and experimental CO desorption energies from Ref. 7. Surface energies are per surface-plane atom. (b) Exchange enhancement factors of

J. Sun *et al.*, Phys. Rev. B 83, 12140(R) (2011).

Van der Waals-DFT

$$E_c^{\mathrm{nl}} = \int \int \rho(\mathbf{r})\phi(\mathbf{r},\mathbf{r}')\rho(\mathbf{r}')d\mathbf{r}d\mathbf{r}'$$

Prism

Cage

Book

Cyclic

Hybrid functionals Fazit

$$E_{xc}^{hyb.} = aE_X^{HF} + (1-a)E_X^{DFT} + E_c^{DFT}$$

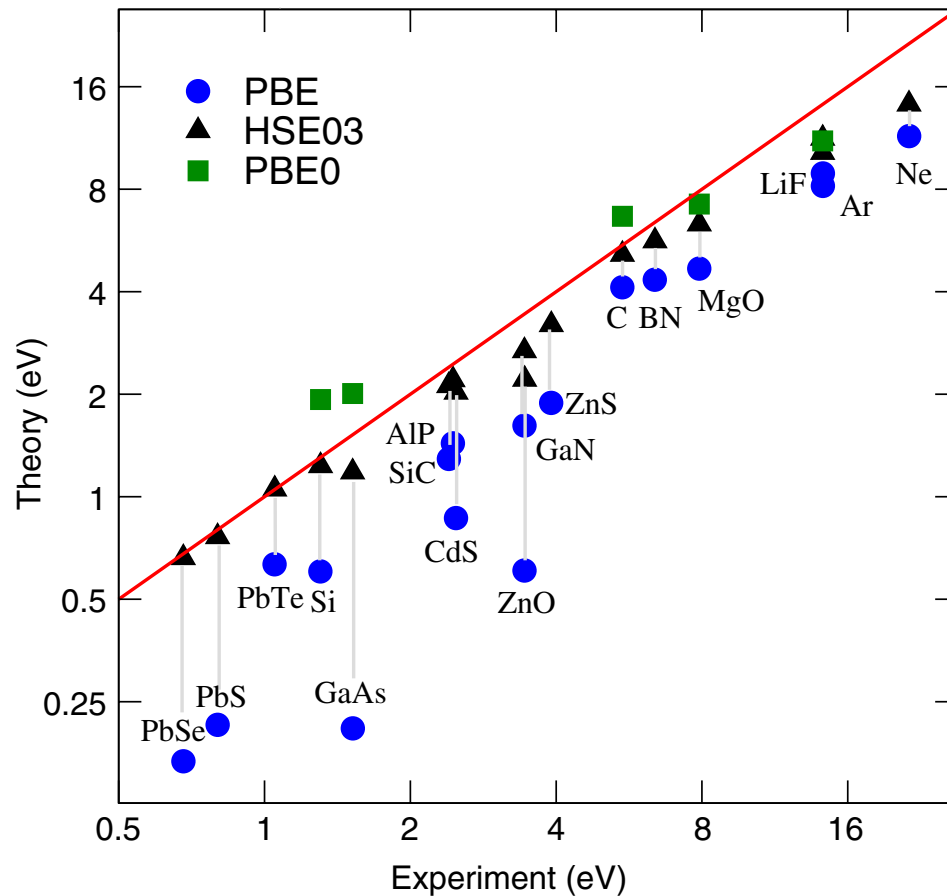**Figure 8.** Band gaps from PBE, PBE0, and HSE03 calculations, plotted against data from experiment.

Lattice constant		
	MRE	MARE
PBE	0.8	1.0
PBE0	0.1	0.5
HSE	0.2	0.5
B3LYP	1.0	1.2

Bulk modulus		
	MRE	MARE
PBE	-9.8	9.4
PBE0	-1.2	5.7
HSE	-3.1	6.4
B3LYP	-10.2	11.4

Atomization energy		
	MRE	MARE
PBE	-1.9	3.4
PBE0	-6.5	7.4
HSE	-5.1	6.3
B3LYP	-17.6	17.6

CO adsorption on d-metal surfaces (cont. I)

CO @		top	fcc	hcp	Δ
Cu(111)	PBE	0.709	0.874	0.862	−0.165
	PBE0	0.606	0.579	0.565	0.027
	HSE03	0.561	0.555	0.535	0.006
	exp.	0.46-0.52			
Rh(111)	PBE	1.870	1.906	1.969	−0.099
	PBE0	2.109	2.024	2.104	0.005
	HSE03	2.012	1.913	1.996	0.016
	exp.	1.43-1.65			
Pt(111)	PBE	1.659	1.816	1.750	−0.157
	PBE0	1.941	1.997	1.944	−0.056
	HSE03	1.793	1.862	1.808	−0.069
	exp.	1.43-1.71			

CO adsorption on d-metal surfaces (cont. II)

Hybrid functionals reduce the tendency to stabilize adsorption at the hollow sites w.r.t. the top site.

Reduced CO $2\pi^*$ $\longleftrightarrow$ metal-d interaction

- Improved description of the CO LUMO ($2\pi^*$) w.r.t. the Fermi level (shifted upwards).
- Downshift of the metal d-band center of gravity in Cu(111).
- But: Overestimation of the metal d-bandwidth.

A. Stroppa, K. Termentzidis, J. Paier, G. Kresse, and J. Hafner, Phys. Rev. B 76, 195440 (2007).
A. Stroppa and G. Kresse, New Journal of Physics 10, 063020 (2008).

One-electron picture

DFT: Kohn-Sham eq.

$$\left(-\frac{1}{2}\Delta + V_{\text{ext}}(\mathbf{r}) + V_{\text{H}}(\mathbf{r}) + V_{\text{xc}}(\mathbf{r})\right)\psi_{n\mathbf{k}}(\mathbf{r}) = \epsilon_{n\mathbf{k}}\psi_{n\mathbf{k}}(\mathbf{r})$$

DFT-HF hybrid functionals: Roothaan eq.

$$\left(-\frac{1}{2}\Delta + V_{\text{ext}}(\mathbf{r}) + V_{\text{H}}(\mathbf{r})\right)\psi_{n\mathbf{k}}(\mathbf{r}) + \int V_{\text{X}}(\mathbf{r},\mathbf{r}')\psi_{n\mathbf{k}}(\mathbf{r}')d\mathbf{r}' = \epsilon_{n\mathbf{k}}\psi_{n\mathbf{k}}(\mathbf{r})$$

GW: quasi-particle eq.

$$\left(-\frac{1}{2}\Delta + V_{\text{ext}}(\mathbf{r}) + V_{\text{H}}(\mathbf{r})\right)\psi_{n\mathbf{k}}(\mathbf{r}) + \int \Sigma(\mathbf{r},\mathbf{r}',E_{n\mathbf{k}})\psi_{n\mathbf{k}}(\mathbf{r}')d\mathbf{r}' = E_{n\mathbf{k}}\psi_{n\mathbf{k}}(\mathbf{r})$$

The Green's function

The Green's function is the "inverse" of the Hamiltonian:

$$1 = (\omega - H)G \quad \Longleftrightarrow \quad G^{-1} = (\omega - H)$$

The Green's function of a Kohn-Sham (non-interacting) Hamiltonian is given by:

$$G_0(\mathbf{r}, \mathbf{r}', \omega) = \sum_n \frac{\psi_n(\mathbf{r})\psi_n^*(\mathbf{r}')}{\omega - \epsilon_n + i\eta \, \mathrm{sgn}(\epsilon_n - \mu)}$$

and the Green's function of an interacting Hamiltonian:

non-int.

$$\left(-\frac{\hbar^2}{2m_e}\Delta + V_{\mathrm{ion}}(\mathbf{r}) + V_{\mathrm{H}}(\mathbf{r})\right) + \Sigma(\mathbf{r}, \mathbf{r}', \omega) = H(\omega) \quad \Longrightarrow \quad H_0 + \Sigma(\omega) = H(\omega)$$

energy/frequency dependent Hamiltonian

$$(H_0 - \omega) + \Sigma(\omega) = (H - \omega)$$

$$-G_0^{-1}(\omega) + \Sigma(\omega) = -G^{-1}(\omega)$$

"Dyson-equation"

$$G^{-1}(\omega) = G_0^{-1}(\omega) - \Sigma(\omega) \Longleftrightarrow G(\omega) = G_0(\omega) + G_0(\omega)\Sigma(\omega)G(\omega)$$

The Green's function: physical interpretation

- The Green's function $G(\mathbf{r}, \mathbf{r}', t - t')$ describes the propagation of a particle from $(\mathbf{r}, t)$ to $(\mathbf{r}', t)$: i.e., provided we have particle at position $\mathbf{r}$ at time t, $G(\mathbf{r}, \mathbf{r}', t - t')$ is the chance of finding it at position $\mathbf{r}'$ at time t'.

$$G_0(\mathbf{r}, \mathbf{r}', \omega) = \sum_n^{\text{all}} \frac{\psi_n^*(\mathbf{r})\psi_n(\mathbf{r}')}{\omega - \epsilon_n + i\eta \, \text{sgn}(\epsilon_n - \mu)}$$

- Particle propagator: $G_o(1,2) = G_o(\mathbf{r}_1, \mathbf{r}_2, t_2 - t_1)$ for $t_2 > t_1$:

$(\mathbf{r}_1, t_1) = 1 \qquad (\mathbf{r}_2, t_2) = 2$

$$G_0(1, 2) = \sum_n^{\text{vir.}} \psi_n(\mathbf{r}_1)^* \psi_n(\mathbf{r}_2) e^{-i(\epsilon_n - \mu)(t_2 - t_1)}$$

- Hole propagator: $G_o(1,2)$ for $t_1 > t_2$:

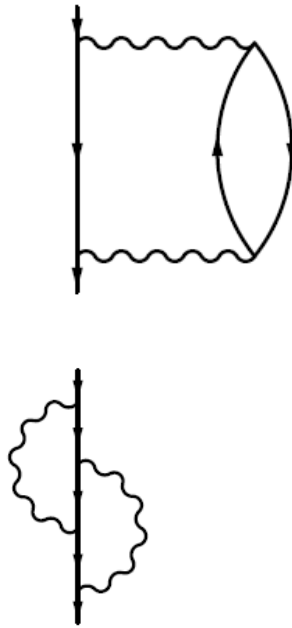$(\mathbf{r}_2, t_2) = 2 \qquad (\mathbf{r}_1, t_1) = 1$

$$G_0(1, 2) = \sum_n^{\text{occ.}} \psi_n^*(\mathbf{r}_1) \psi_n(\mathbf{r}_2) e^{-i(\epsilon_n - \mu)(t_1 - t_2)}$$

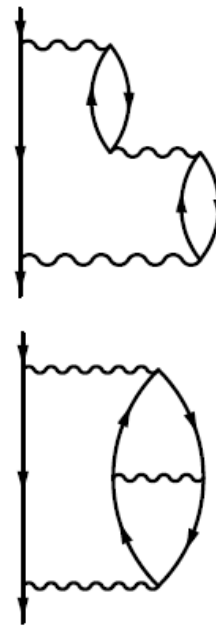# Perturbation theory: Σ as a function of *G*

- The selfenergy Σ, is made up of all Feynman diagrams with one in- and one out-going propagator line:
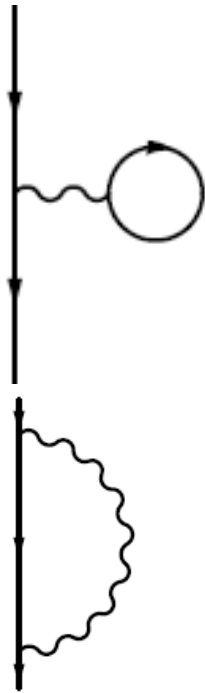
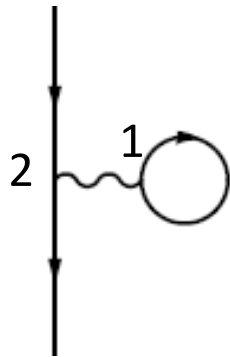

1st. order   2nd. order   3rd. order   4th. order

- And many, many, many, more

Perturbation theory: Σ as a function of G

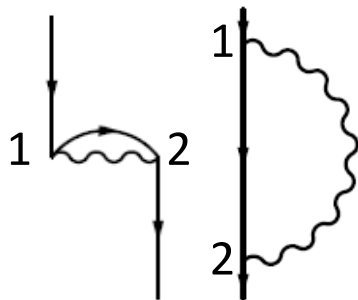The two first-order diagrams represent the Hartree and exchange interaction:

Hartree

$$G_0(1,1) = \sum_n^{\text{occ.}} \psi_n(\mathbf{r}_1)^* \psi_n(\mathbf{r}_1) e^{-i(\epsilon_n - \mu)(t_1 - t_1)} = n(\mathbf{r}_1)$$

$$\nu(2,1)G_0(1,1) = \int \nu(\mathbf{r}_2, \mathbf{r}_1) n(\mathbf{r}_1) d\mathbf{r}_1 = \int \frac{n(\mathbf{r}_1)}{|\mathbf{r}_1 - \mathbf{r}_2|} d\mathbf{r}_1$$
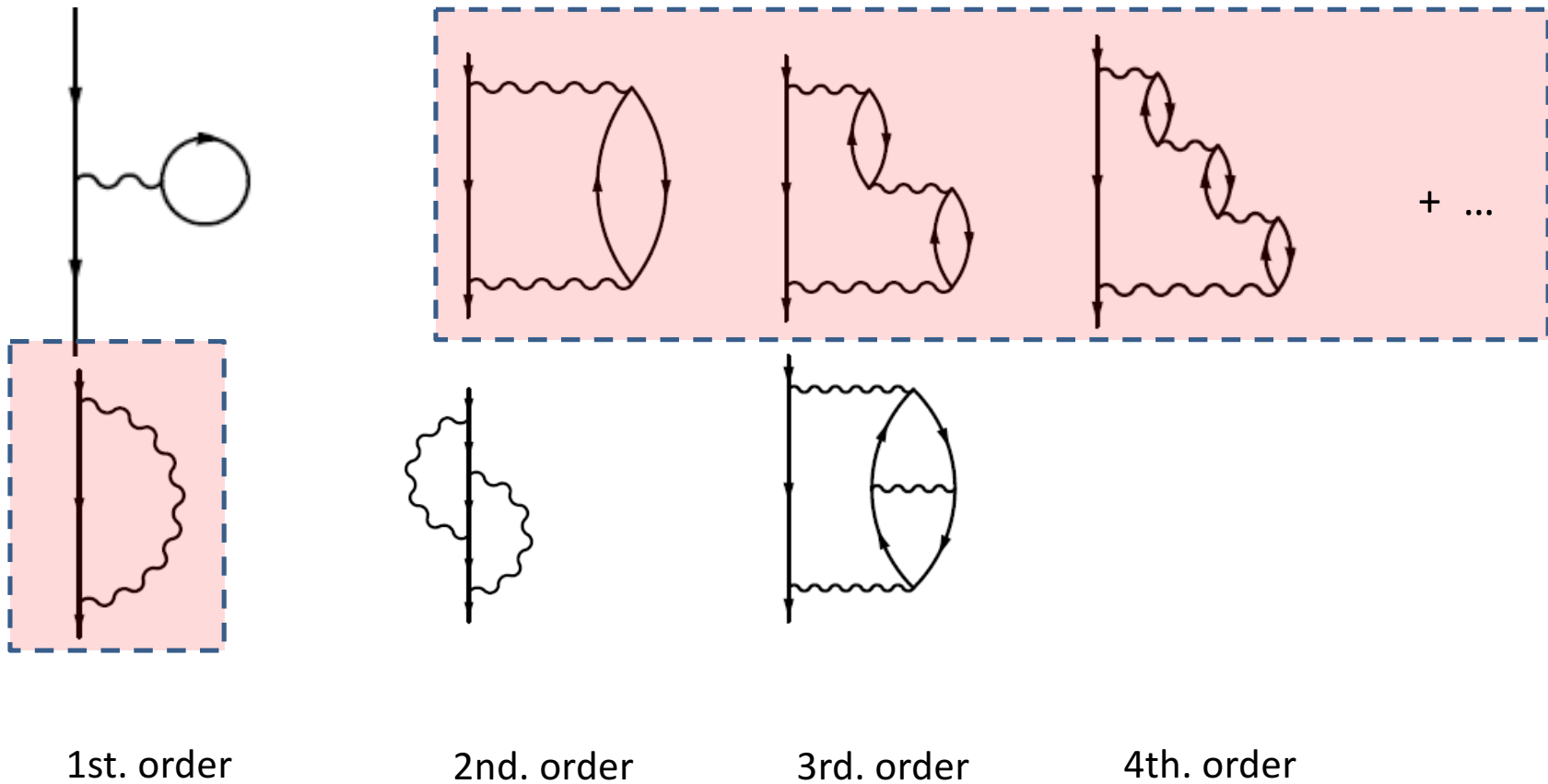
Exchange

$$G_0(1,2) = \sum_n^{\text{occ.}} \psi_n(\mathbf{r}_1)^* \psi_n(\mathbf{r}_2) e^{-i(\epsilon_n - \mu)(t_1 - t_1)} = \gamma(\mathbf{r}_1, \mathbf{r}_2)$$

$$-G_0(1,2)\nu(1,2) = -\nu(\mathbf{r}_1, \mathbf{r}_2)\gamma(\mathbf{r}_1, \mathbf{r}_2) = \frac{\gamma(\mathbf{r}_1, \mathbf{r}_2)}{|\mathbf{r}_1 - \mathbf{r}_2|}$$
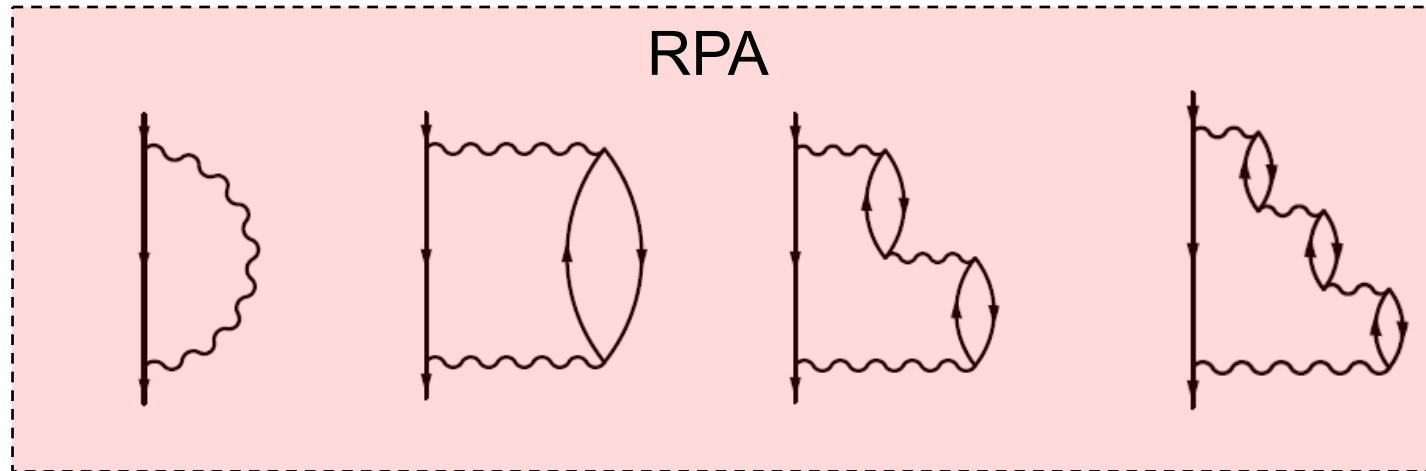
Perturbation theory: Σ as a function of *G*

- Some diagrams are easier to calculate than others.
  Random-Phase-Approximation (RPA):

1st. order   2nd. order   3rd. order   4th. order

The screened Coulomb interaction: W

- These diagrams can be expressed as a screened Coulomb interaction, W:

$$W = \epsilon^{-1}\nu \qquad \epsilon^{-1} = 1 + \nu\chi \qquad \chi = \chi^0 + \chi^0\nu\chi$$
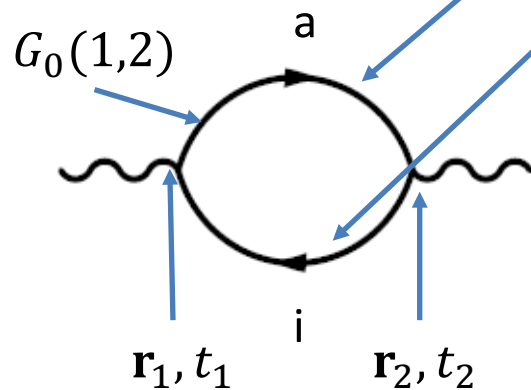
The IP-polarizability: χ_0

The "irreducible polarizability in the independent particle picture" χ^0 (or χ^{KS}):

$$\chi^0(\mathbf{r}, \mathbf{r}', \omega) := \frac{\partial \rho_{\text{ind}}(\mathbf{r}, \omega)}{\partial v_{\text{eff}}(\mathbf{r}', \omega)}$$

Adler and Wiser derived expressions for χ^0

$$\chi_0(\mathbf{r}_1, \mathbf{r}_2, \omega) = \sum_i^{\text{occ.}} \sum_a^{\text{virt.}} \frac{\langle \psi_a | \mathbf{r}_1 | \psi_i \rangle \langle \psi_i | \mathbf{r}_2 | \psi_a \rangle}{\epsilon_i - \epsilon_a - \omega} + \sum_i^{\text{occ.}} \sum_a^{\text{virt.}} \frac{\langle \psi_i | \mathbf{r}_1 | \psi_a \rangle \langle \psi_a | \mathbf{r}_2 | \psi_i \rangle}{\epsilon_a - \epsilon_i - \omega}$$

$G_0(1,2)$

a

i

$\mathbf{r}_1, t_1$ $\mathbf{r}_2, t_2$

Or in terms of Green's functions (propagators):

$$\chi_0(\mathbf{r}_1, t_1, \mathbf{r}_2, t_2) = \chi(1, 2) = -G_0(1, 2) G_0(2, 1)$$

The IP-polarizability: χ_0

And in terms of Block functions χ^0 can be written as

$$\chi^0_{\mathbf{G},\mathbf{G'}}(\mathbf{q},\omega) = \frac{1}{\Omega} \sum_{nn'\mathbf{k}} 2w_{\mathbf{k}}(f_{n'\mathbf{k}+\mathbf{q}} - f_{n'\mathbf{k}})$$

$$\times \frac{\langle\psi_{n'\mathbf{k}+\mathbf{q}}|e^{i(\mathbf{q}+\mathbf{G})\mathbf{r}}|\psi_{n\mathbf{k}}\rangle\langle\psi_{n\mathbf{k}}|e^{-i(\mathbf{q}+\mathbf{G'})\mathbf{r'}}|\psi_{n'\mathbf{k}+\mathbf{q}}\rangle}{\epsilon_{n'\mathbf{k}+\mathbf{q}} - \epsilon_{n\mathbf{k}} - \omega - i\eta}$$

Expensive: computing the IP-polarizability scales as N^4

Once we have χ^0 the screened Coulomb interaction (in the RPA) is computed as:

$$W = \nu + \nu\chi_0\nu + \nu\chi_0\nu\chi_0\nu + \nu\chi_0\nu\chi_0\nu\chi_0\nu + \ldots = \nu \underbrace{(1 - \chi_0\nu)^{-1}}_{\epsilon^{-1}}$$

geometrical series

1. The bare Coulomb interaction between two particles

2. The electronic environment reacts to the field generated by a particle: induced change in the density $\chi_0\nu$, that gives rise to a change in the Hartree potential: $\nu\chi_0\nu$.

3. The electrons react to the induced change in the potential: additional change in the density, $\chi_0\nu\chi_0\nu$, and corresponding change in the Hartree potential: $\nu\chi_0\nu\chi_0\nu$.

and so on, and so on …

GW

The quasi-particle equation:

$$\left(-\frac{1}{2}\Delta + V_{\text{ext}}(\mathbf{r}) + V_{\text{H}}(\mathbf{r})\right)\psi_{n\mathbf{k}}(\mathbf{r}) + \int \Sigma(\mathbf{r},\mathbf{r}',E_{n\mathbf{k}})\psi_{n\mathbf{k}}(\mathbf{r}')d\mathbf{r}' = E_{n\mathbf{k}}\psi_{n\mathbf{k}}(\mathbf{r})$$

The "self-energy is given by:

$$\Sigma = iGW$$

Green's function: G

or more explicitly

$$\Sigma(\mathbf{r},\mathbf{r}',E) = \frac{i}{2\pi}\int_{-\infty}^{\infty}d\omega \sum_n^{\text{all}} \frac{\psi_n(\mathbf{r})\psi_n^*(\mathbf{r}')}{\omega - E - E_n + i\eta\,\text{sgn}(E_n - E_{\text{fermi}})} \times$$

$$\times e^2 \int d\mathbf{r}'' \frac{\epsilon^{-1}(\mathbf{r},\mathbf{r}'',\omega)}{|\mathbf{r}'' - \mathbf{r}'|}$$
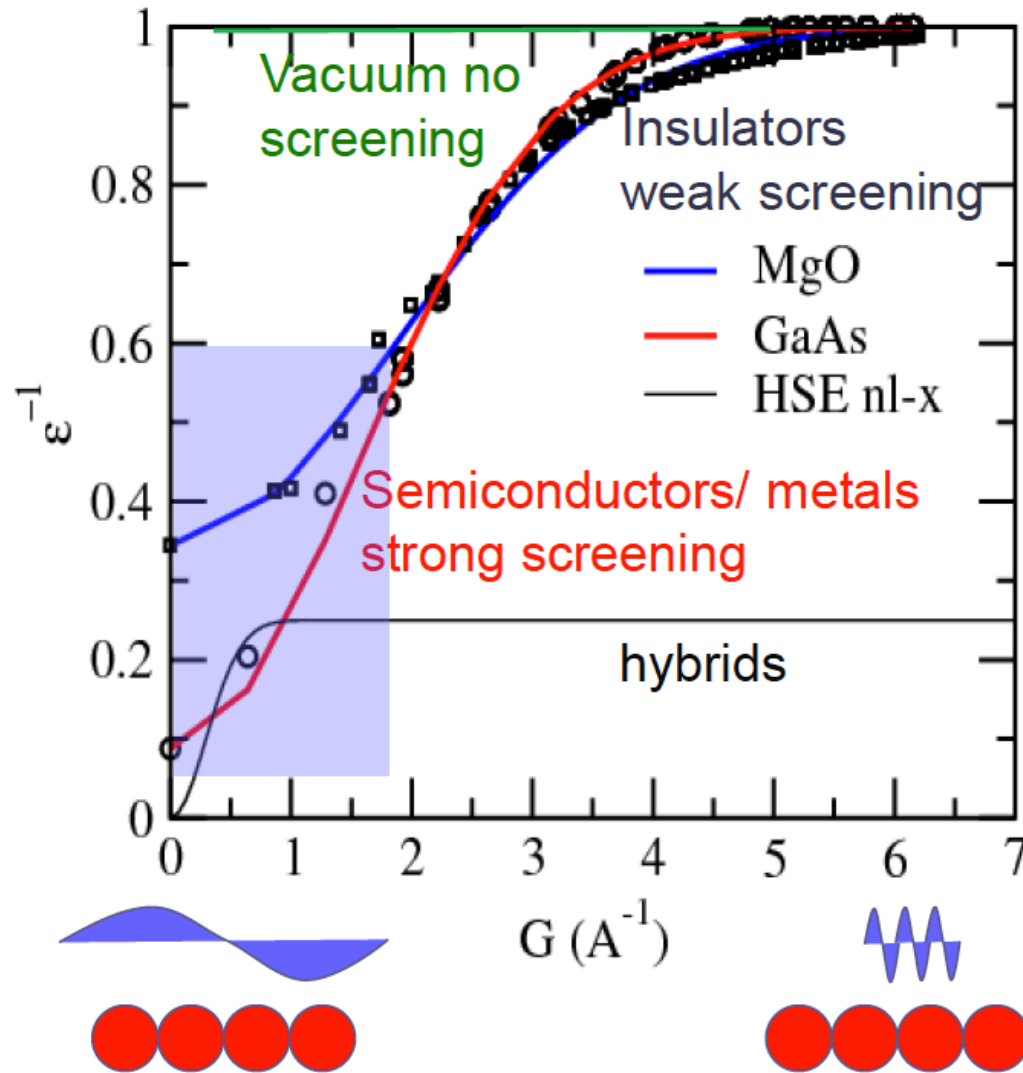
screened Coulomb interaction: W

Compare to Fock-exchange:

$$V_{\text{X}}(\mathbf{r},\mathbf{r}') = -\sum_n^{\text{occ.}} \psi_n(\mathbf{r})\psi_n^*(\mathbf{r}') \times \frac{e^2}{|\mathbf{r} - \mathbf{r}'|}$$

bare Coulomb interaction: v

An analogy between GW and hybrid functionals

- $\epsilon^{-1}(G)$:
  Strong screening for small G (static screening properties).

  No screening at large G.

  Screening is system dependent, obviously.

- Hybrids: ¼ is a compromise, that works well for small-to-medium gap systems.

Spectral representation of χ_0

It is cheaper to calculate the polarizability in its spectral representation

$$\chi^S_{\mathbf{G},\mathbf{G}'}(\mathbf{q},\omega') = \frac{1}{\Omega} \sum_{nn'\mathbf{k}} 2w_{\mathbf{k}} \, \text{sgn}(\omega')\delta(\omega' + \epsilon_{n\mathbf{k}} - \epsilon_{n'\mathbf{k}-\mathbf{q}})(f_{n\mathbf{k}} - f_{n'\mathbf{k}-\mathbf{q}}) \times$$

$$\times \langle\psi_{n\mathbf{k}}|e^{i(\mathbf{q}+\mathbf{G})\mathbf{r}}|\psi_{n'\mathbf{k}-\mathbf{q}}\rangle\langle\psi_{n'\mathbf{k}-\mathbf{q}}|e^{-i(\mathbf{q}+\mathbf{G})\mathbf{r}}|\psi_{n\mathbf{k}}\rangle$$

which is related to the imaginary part of χ_0 through

$$\chi^S_{\mathbf{G},\mathbf{G}'}(\mathbf{q},\omega') = \frac{1}{\pi}\Im\left[\chi^0_{\mathbf{G},\mathbf{G}'}(\mathbf{q},\omega)\right]$$

The polarizability χ_0 is then obtained from its spectral representation through the following Hilbert transform

$$\chi^0_{\mathbf{G},\mathbf{G}'}(\mathbf{q},\omega) = \int_0^\infty d\omega' \chi^S_{\mathbf{G},\mathbf{G}'}(\mathbf{q},\omega') \times \left(\frac{1}{\omega - \omega' - i\eta} - \frac{1}{\omega + \omega' + i\eta}\right)$$

`LSPECTRAL=.TRUE.|.FALSE.`   `NOMEGA=[integer]`
(Default for ALGO = CHI | GW0 | GW | scGW0 | scGW, when NOMEGA>2)

Solving the GW QP-equation

$$\left(-\frac{1}{2}\Delta + V_{\text{ext}}(\mathbf{r}) + V_{\text{H}}(\mathbf{r}) \right) \psi_{n\mathbf{k}}(\mathbf{r}) + \int \Sigma(\mathbf{r}, \mathbf{r}', E_{n\mathbf{k}})\psi_{n\mathbf{k}}(\mathbf{r}')d\mathbf{r}' = E_{n\mathbf{k}}\psi_{n\mathbf{k}}(\mathbf{r})$$

The quasi-particle energies are given by

$$E_{n\mathbf{k}} = \Re\left[\langle \psi_{n\mathbf{k}}| - \frac{1}{2}\Delta + V_{\text{ext}} + V_{\text{H}} + \Sigma(E_{n\mathbf{k}})|\psi_{n\mathbf{k}}\rangle \right]$$

which may be solved by iteration

$$E_{n\mathbf{k}}^{N+1} = \Re\left[\langle \psi_{n\mathbf{k}}| - \frac{1}{2}\Delta + V_{\text{ext}} + V_{\text{H}} + \Sigma(E_{n\mathbf{k}}^{N})|\psi_{n\mathbf{k}}\rangle \right]$$

$$+ (E_{n\mathbf{k}}^{N+1} - E_{n\mathbf{k}}^{N})\Re\left[\langle \psi_{n\mathbf{k}}|\frac{\partial\Sigma(\omega)}{\partial\omega}\Big|_{\omega=E_{n\mathbf{k}}^{N}}|\psi_{n\mathbf{k}}\rangle \right]$$

$$= E_{n\mathbf{k}}^{N} + Z_{n\mathbf{k}}^{N}\Re\left[\langle \psi_{n\mathbf{k}}| - \frac{1}{2}\Delta + V_{\text{ext}} + V_{\text{H}} + \Sigma(E_{n\mathbf{k}}^{N})|\psi_{n\mathbf{k}}\rangle - E_{n\mathbf{k}}^{N} \right]$$

where

$$Z_{n\mathbf{k}}^{N} = \left(1 - \langle \psi_{n\mathbf{k}}|\frac{\partial\Sigma(\omega)}{\partial\omega}\Big|_{\omega=E_{n\mathbf{k}}^{N}}|\psi_{n\mathbf{k}}\rangle \right)^{-1}$$

Single shot GW: $G_0 W_0$

- Calculate DFT orbitals:

$$\left(-\frac{1}{2}\Delta + V_{\text{ext}}(\mathbf{r}) + V_{\text{H}}(\mathbf{r}) + V_{\text{xc}}(\mathbf{r}) \right) \psi_{n\mathbf{k}}(\mathbf{r}) = \epsilon_{n\mathbf{k}} \psi_{n\mathbf{k}}(\mathbf{r})$$

- Compute G_o, W_o, and $\Sigma = G_0 W_0$ from the DFT orbitals and eigenenergies.
- Determine the first-order change in the eigenenergies:

$$E_{n\mathbf{k}} = \Re \left[\langle \psi_{n\mathbf{k}} | -\frac{1}{2}\Delta + V_{\text{ext}} + V_{\text{H}} + \Sigma(\epsilon_{n\mathbf{k}}) | \psi_{n\mathbf{k}} \rangle \right]$$

- Actually the expression above is linearized and in single-shot GW ($G_0 W_0$) we evaluate:

$$E_{n\mathbf{k}} = \epsilon_{n\mathbf{k}} + Z_{n\mathbf{k}} \Re \left[\langle \psi_{n\mathbf{k}} | -\frac{1}{2}\Delta + V_{\text{ext}} + V_{\text{H}} + \Sigma(\epsilon_{n\mathbf{k}}) | \psi_{n\mathbf{k}} \rangle - \epsilon_{n\mathbf{k}} \right]$$

where

$$Z_{n\mathbf{k}}^N = \left(1 - \langle \psi_{n\mathbf{k}} | \frac{\partial \Sigma(\omega)}{\partial \omega} \Big|_{\omega = E_{n\mathbf{k}}^N} | \psi_{n\mathbf{k}} \rangle \right)^{-1}$$

The GW_0 approximation

- Calculate DFT orbitals:

$$\left(-\frac{1}{2}\Delta + V_{\text{ext}}(\mathbf{r}) + V_{\text{H}}(\mathbf{r}) + V_{\text{xc}}(\mathbf{r}) \right) \psi_{n\mathbf{k}}(\mathbf{r}) = \epsilon_{n\mathbf{k}} \psi_{n\mathbf{k}}(\mathbf{r})$$

- Compute G_o, W_o, and $\Sigma = G_0 W_0$ from the DFT orbitals and eigenenergies.
- Determine the first-order change in the eigenenergies:

$$E_{n\mathbf{k}} = \Re \left[\langle \psi_{n\mathbf{k}} | -\frac{1}{2}\Delta + V_{\text{ext}} + V_{\text{H}} + \Sigma(\epsilon_{n\mathbf{k}}) | \psi_{n\mathbf{k}} \rangle \right]$$
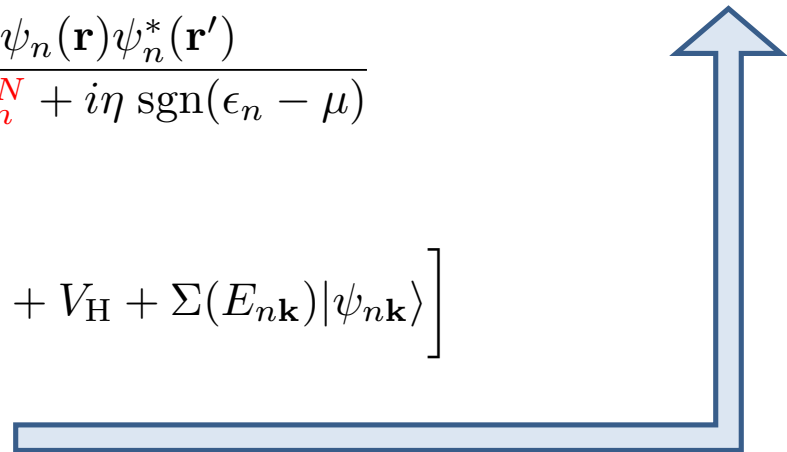
- And recompute the Green's function using the QP-energies of the previous step:

$$G^N(\mathbf{r}, \mathbf{r}', \omega) = \sum_n \frac{\psi_n(\mathbf{r})\psi_n^*(\mathbf{r}')}{\omega - E_n^N + i\eta \, \text{sgn}(\epsilon_n - \mu)}$$
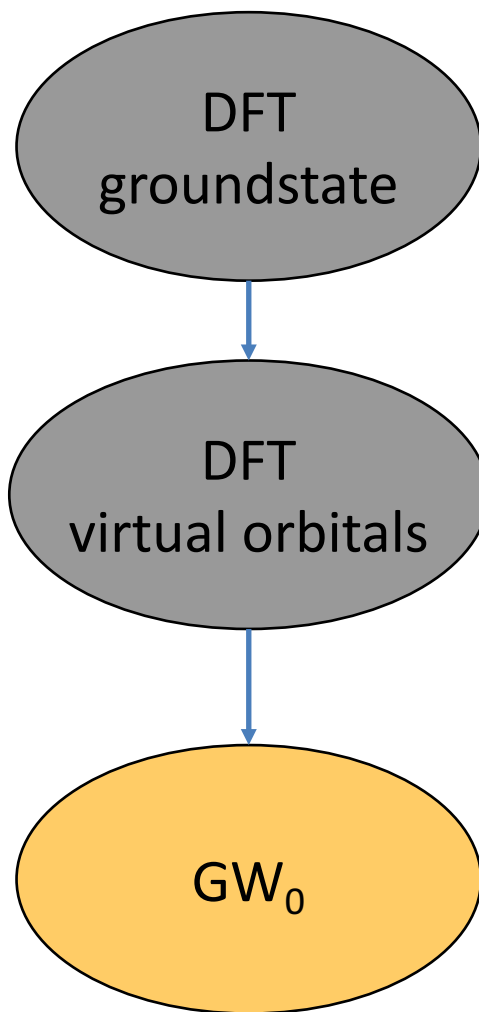
- Compute $\Sigma = GW_0$ and:

$$E_{n\mathbf{k}} = \Re \left[\langle \psi_{n\mathbf{k}} | -\frac{1}{2}\Delta + V_{\text{ext}} + V_{\text{H}} + \Sigma(E_{n\mathbf{k}}) | \psi_{n\mathbf{k}} \rangle \right]$$

- This may be repeated a number of times

G_0W_0 and GW_0 flowchart

DFT groundstate

ISMEAR = 0 ; SIGMA = 0.05
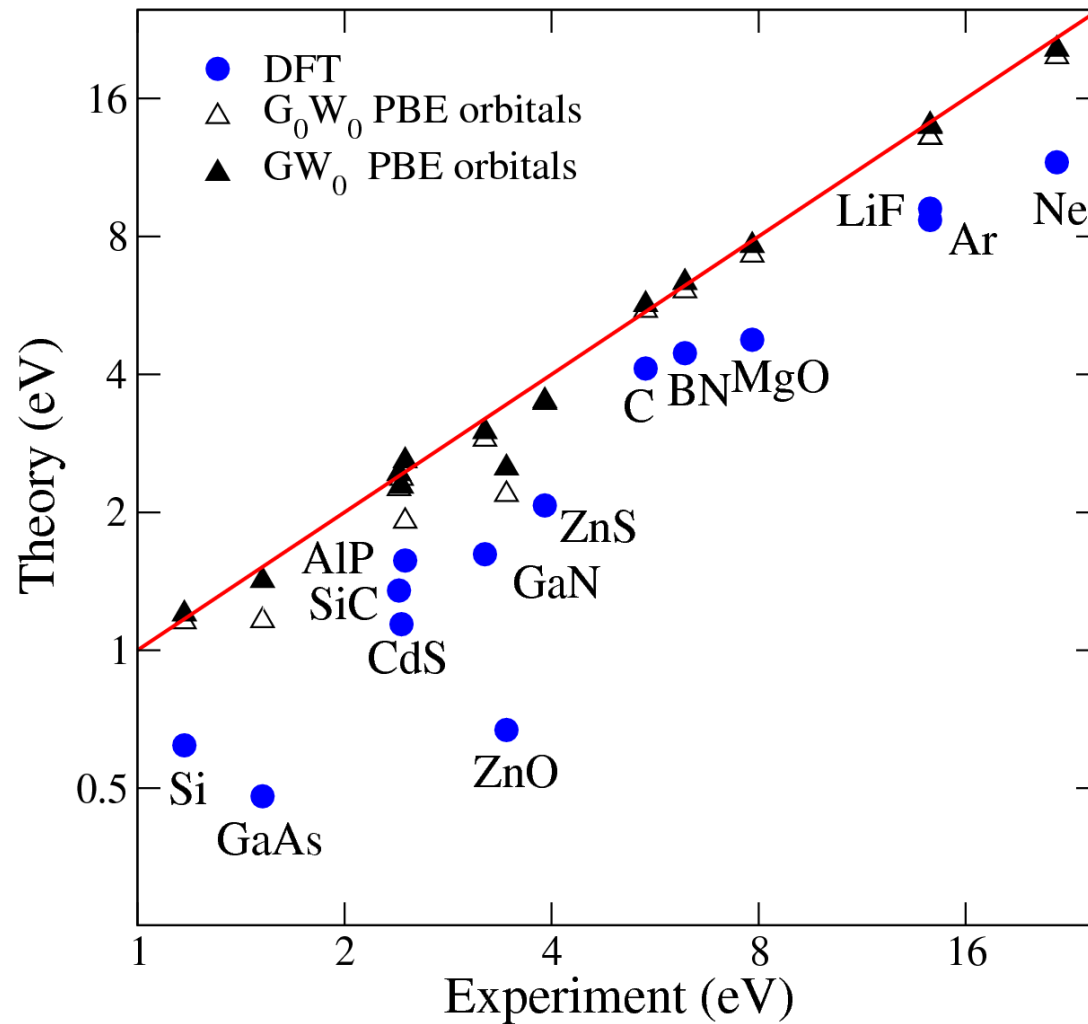EDIFF = 1E-8

DFT virtual orbitals

NBANDS = 50-200 per atom
ALGO = Exact
ISMEAR = 0 ; SIGMA = 0.05
LOPTICS = .TRUE.

GW_0

NBANDS = 50-200 per atom
ALGO = GW0
ISMEAR = 0 ; SIGMA = 0.05
NELM=1   →   G0W0
NELM=4-10   →   converged GW0

Test you could (and should try to) do

- **ENCUT**   Plane wave energy cutoff for orbitals

- **NBANDS**   Total number of bands:
  Try (if possible) to set NBANDS to the total number
  of plane waves.

- **NOMEGA**   Number of frequency points:
  Default: 50 is pretty good, although we often use 100
  Small gap systems might need more freq. points
  little performance penalty (requires more memory).
  Try using 100-200 just to test.

- **ENCUTGW**   Plane wave energy cutoff for response functions:
  Default: 2/3 ENCUT is pretty good.

G0W0(PBE) and GW0 QP-gaps

G_0W_0: MARE 8.5 %
GW_0 : MARE 4.5 %

M. Shishkin, G. Kresse,
PRB **75**, 235102 (2007).

M. Shishkin, M. Marsman,
PRL **95**, 246403 (2007)

A. Grüneis, G. Kresse,
PRL **112**,096401 (2014)

Updating the orbitals: sc-QPGW

To solve for the quasi-particle orbitals we follow the method proposed by Faleev, van Schilfgaarde, and Kotani, Phys. Rev. Lett. 93, 126406 (2004):

- Construct a Hermitian one-electron Hamiltonian approximation to $\Sigma(E)$ and diagonalize that approximate Hamiltonian:
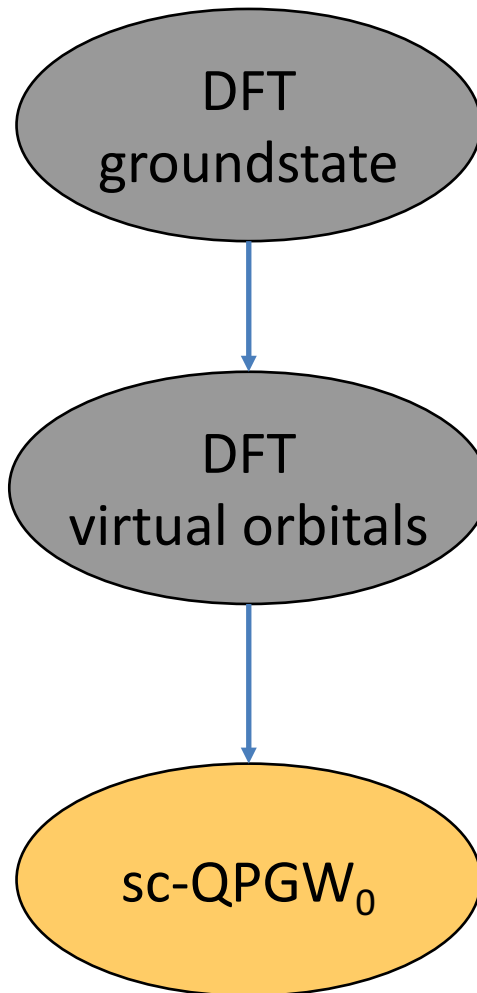
$$(T + V)\,\psi + \Sigma(E)\psi = E\psi$$

$$(T + V)\,\psi + \left[\Sigma(E_0) + \frac{d\Sigma(E_0)}{dE_0}(E - E_0)\right]\psi = E\psi$$

$$(T + V)\,\psi + \left[\Sigma(E_0) - \frac{d\Sigma(E_0)}{dE_0}E_0\right]\psi = E\left[1 - \frac{d\Sigma(E_0)}{dE_0}\right]\psi$$

$$\Sigma^{\mathrm{Herm}}\psi = ES\psi \quad \Longleftrightarrow \quad S^{-1/2}\Sigma^{\mathrm{Herm}}S^{-1/2}\psi' = E\psi'$$
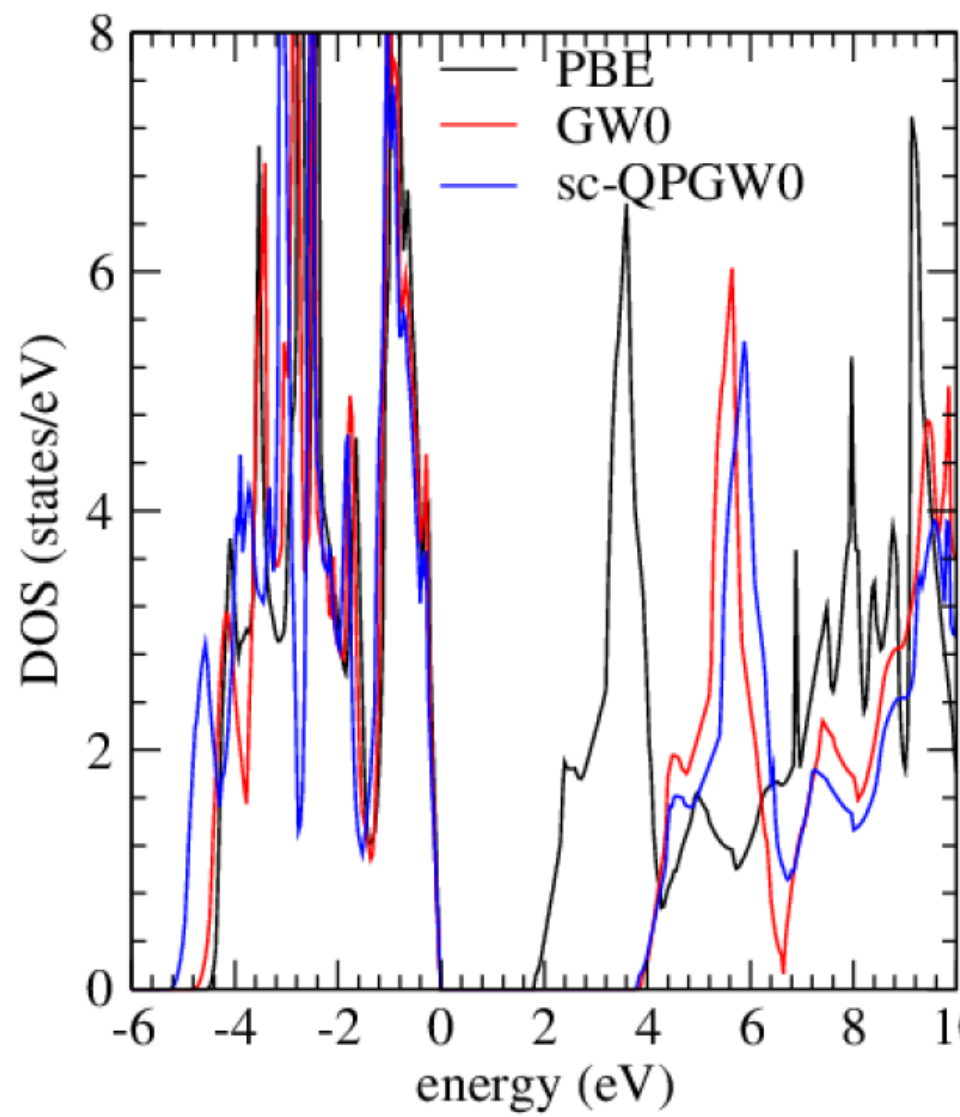
$scQPGW_0$ flowchart
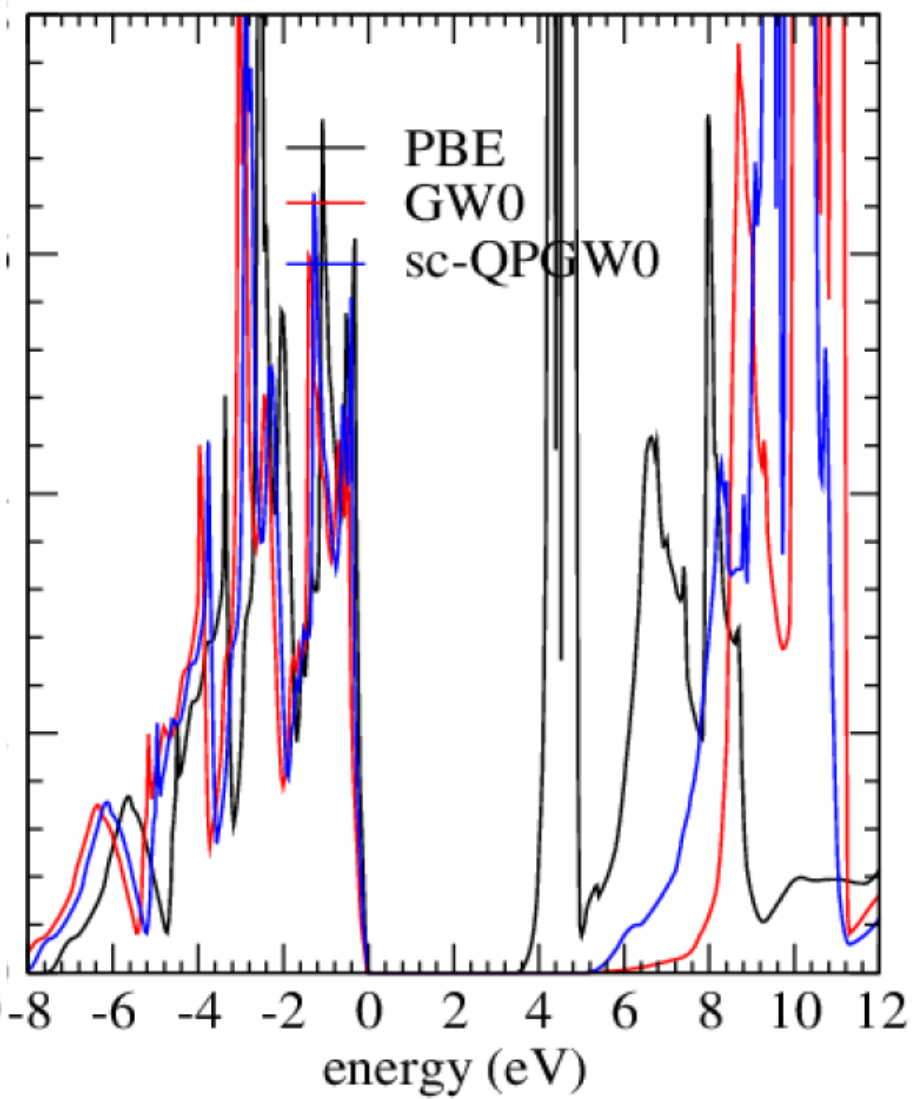
Update the orbitals in G: scGW0
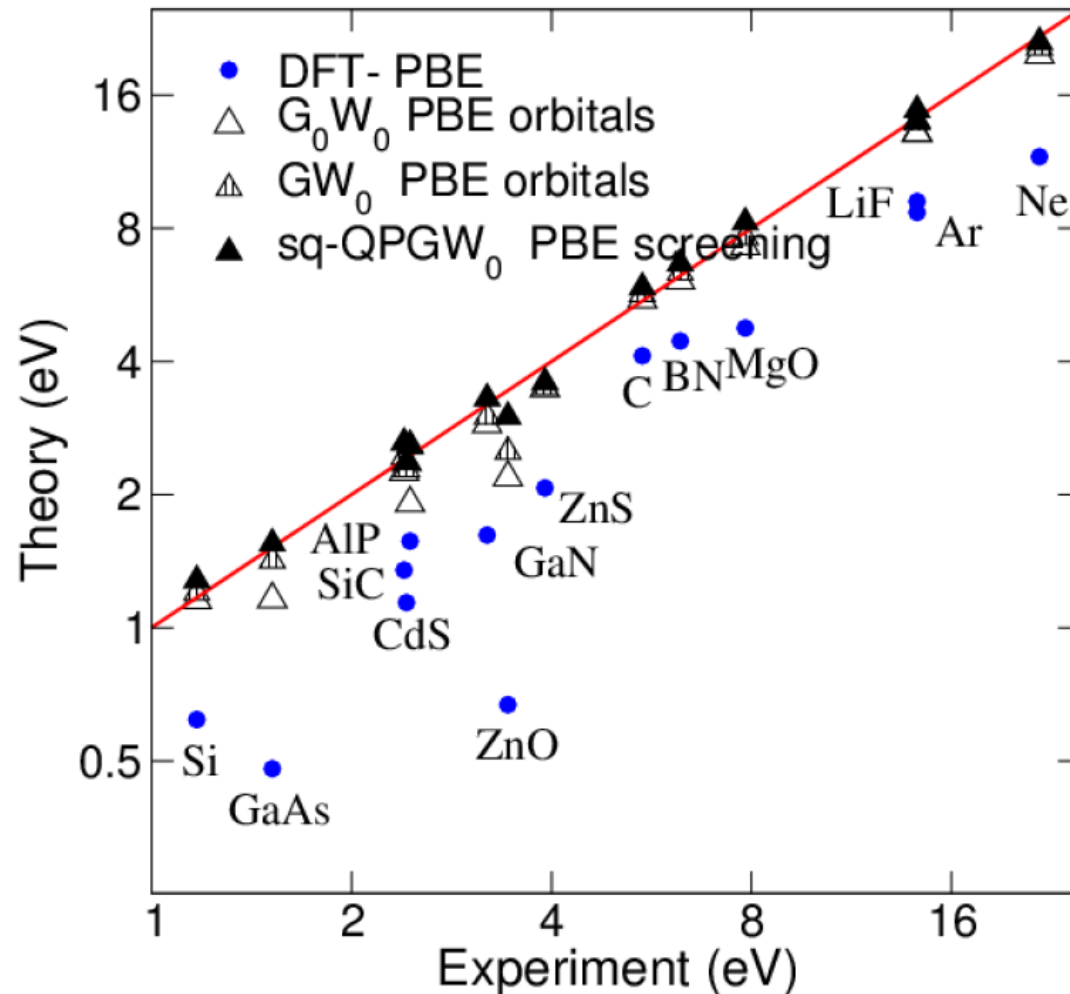
- Little improvement over GW_0

- On average slightly too large gaps

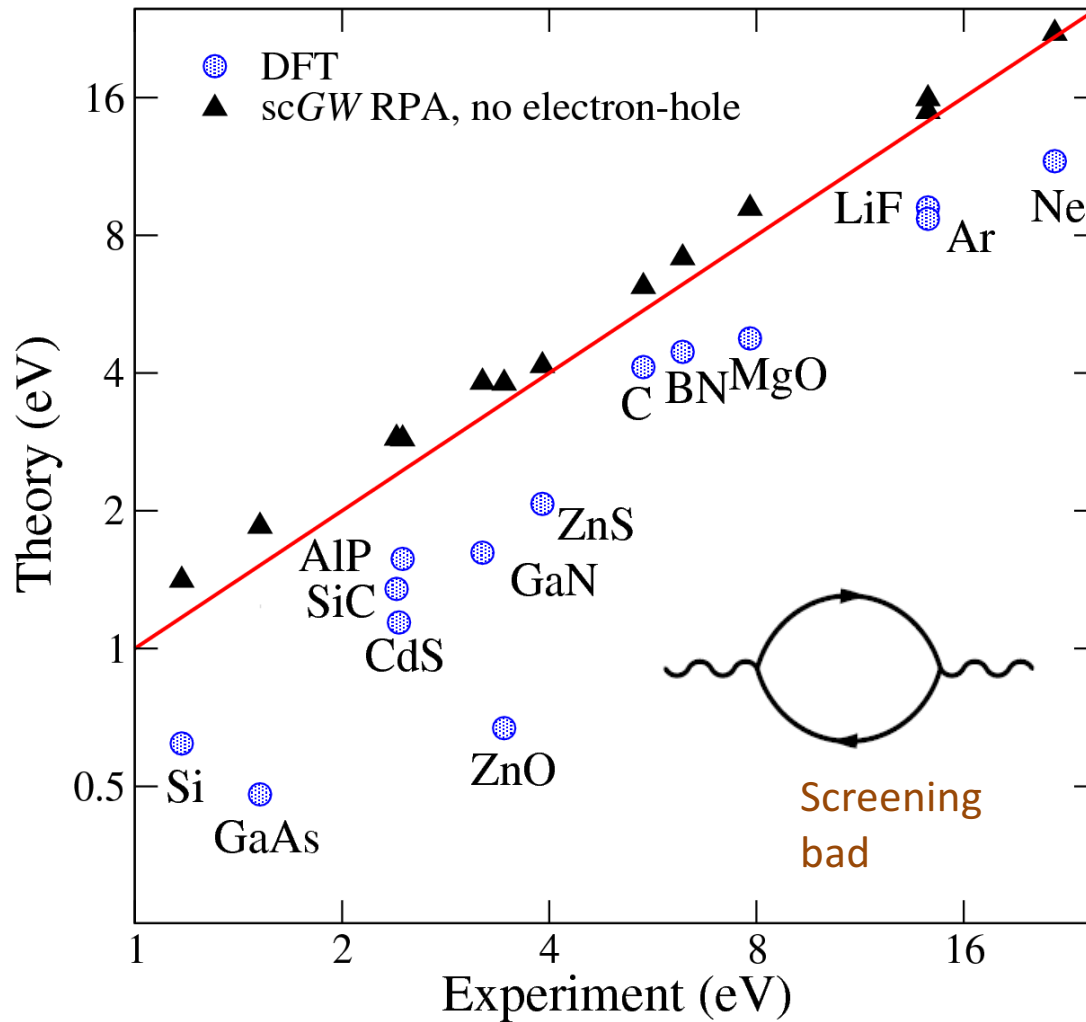M. Shishkin, M. Marsman, PRL 95, 246403 (2007)

BaTiO$_3$

LaAlO$_3$

Fully self-consistent GW

M. Shishkin, M. Marsman, G. Kresse,
PRL 95, 246403 (2007)

Update G and W:
van Schilfgaarde & Kotani
PRL 96, 226402 (2006)

- Well this is dis-appointing, isn't it ? worse than GW_0

- Static dielectric constants are now too small by 20 %
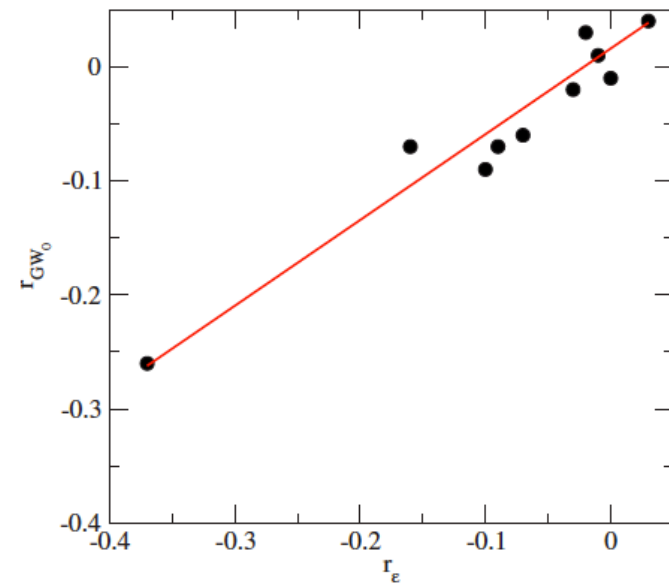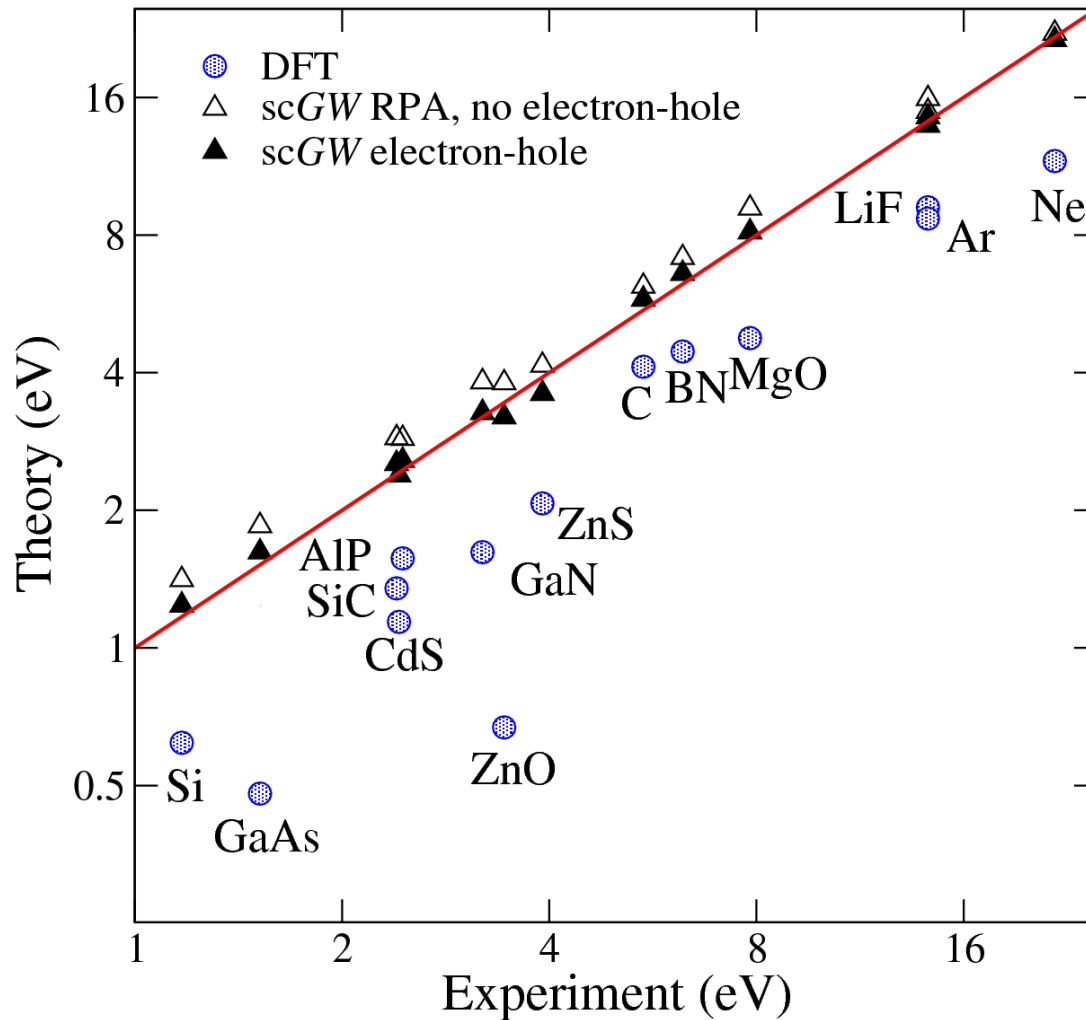
- This is a limitation of the RPA!

FIG. 3. (Color online) Band-gap error r_{GW_0} versus error in the calculated dielectric constants r_ϵ. The line shows a linear fit $r_{GW_0} = 0.01 + 0.75 r_\epsilon$ to all data points.

Fully self-consistent GW
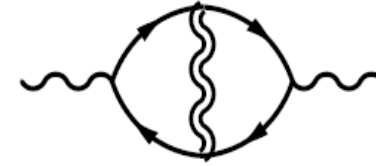
e-h interaction: Nano-quanta kernel (L. Reining)

- Excellent results across all materials: MARE: 3.5 %

- Further slight improvement over GW_0 (PBE)

- Too expensive for large scale applications, but fundamentally important

M. Shishkin, M. Marsman, G. Kresse, PRL 95, 246403 (2007)

Fully self-consistent GW (ϵ_∞)

TABLE II. Theoretical and experimental ion-clamped (high frequency) dielectric constants ε_m. Values with 10% deviation from experiment are underlined. Projector-augmented-wave–DFT values in the independent particle approximation are presented in Ref. [24] alongside other all-electron values.

	scGW RPA	scGW e-h	DFT RPA	EXP
GaAs	8.2	10.4	12.8	11.1
Si	9.2	11.4	12.0	11.9
SiC	5.22	6.48	6.54	6.52
C	5.00	5.58	5.55	5.70
ZnO	2.84	3.78	5.12	3.74
MgO	2.30	2.96	2.99	3.00

Vertex correction include e-h interaction
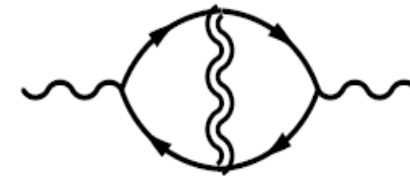
Scaling $N^5 - N^6$

|	Δ (eV)				ε_m	
	scGW RPA	scGW e-h	GW_0^{DFT} RPA	EXP	scGW e-h	EXP
Ge	0.95	0.81	0.75	<u>0.74</u>	15.3	16.2
Si	1.41	1.24	1.28 (1.20)	<u>1.17</u>	11.4	11.9
GaAs	1.85	1.62	1.55 (1.42)	<u>1.52</u>	10.4	11.1
SiC	2.88	2.53	2.62 (2.43)	2.40	6.48	6.52
CdS	2.87	2.39	2.37 (2.28)	2.42	5.31	5.30
AlP	2.90	2.57	2.57 (2.59)	2.45	7.11	7.54
GaN	3.82	3.27	3.30 (3.00)	3.20	5.35	5.30
ZnO	3.8	3.2	3.0 (2.5)	<u>3.44</u>	3.78	3.74
ZnS	4.15	3.60	3.59 (3.50)	<u>3.91</u>	5.15	5.13
C	6.18	5.79	5.88 (5.68)	5.48	5.59	5.70
BN	7.14	6.59	6.66 (6.35)	≈ 6.25	4.43	4.50
MgO	9.16	8.12	8.25 (7.64)	7.83	2.96	3.00
LiF	15.9	14.5	14.8 (14.0)	14.20	1.98	1.90
Ar	14.9	13.9	14.0 (13.9)	14.20	1.69	
Ne	22.1	21.4	21.1 (20.5)	21.70	1.23	
		ϵ_d (eV)				
ZnO		6.7	6.4 (6.4)	7.5–8		
GaAs		17.6	17.3 (17.2)	18.9		

What do we neglect in the RPA

A lot!
We have even neglected one second order diagram, the "second order" exchange
In third order, excitonic effects and many more diagrams have been neglected
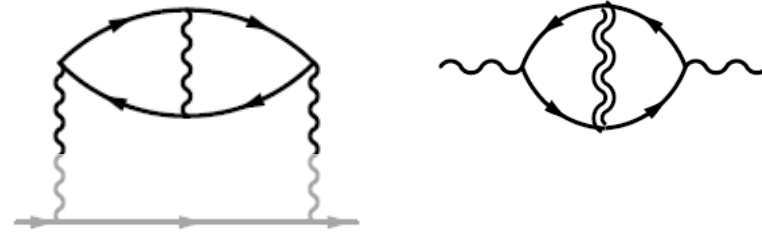

2nd order exchange   exitons

1st. order   2nd. order   3rd. order   4th. order
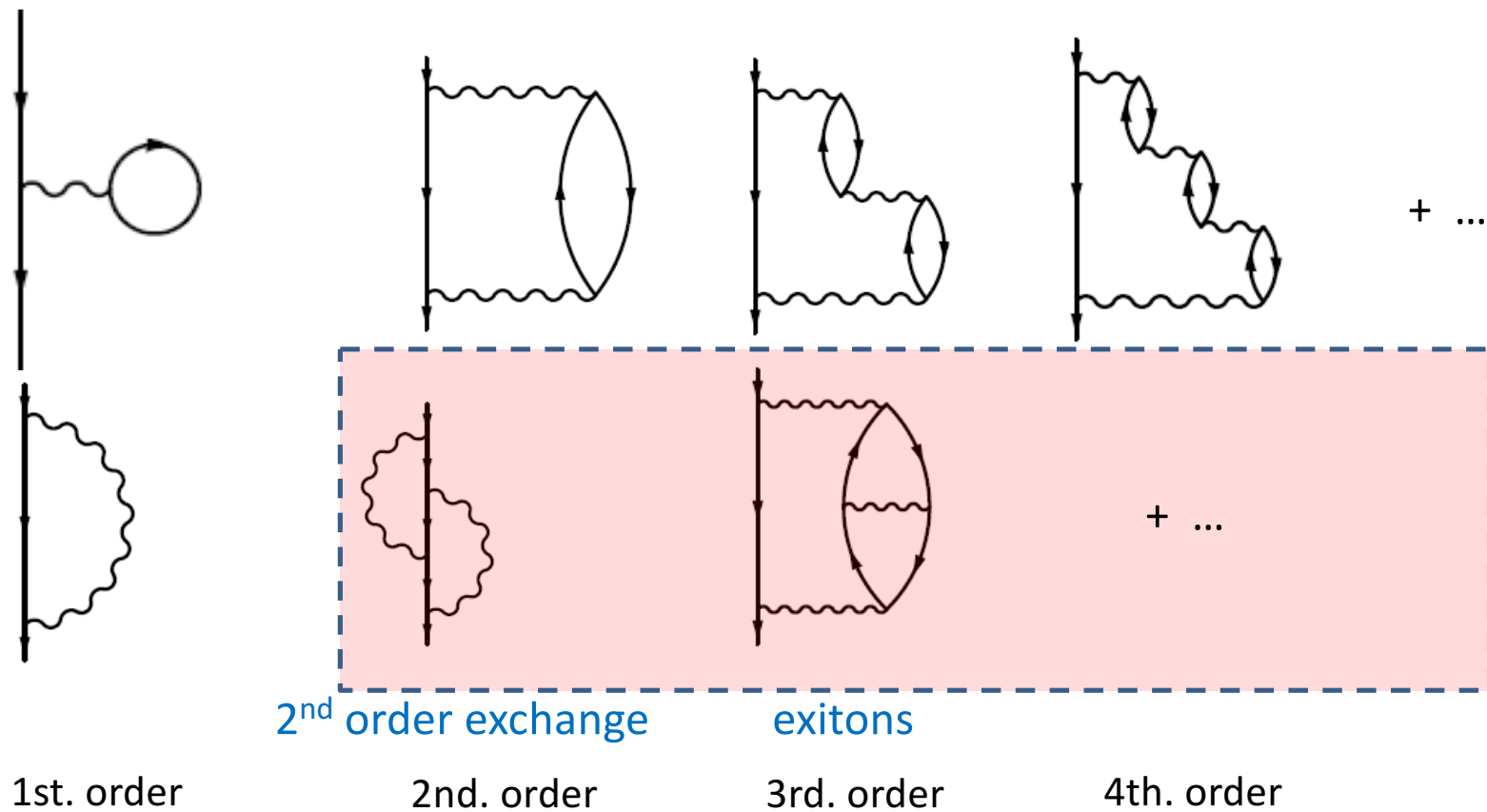
What do we neglect in the RPA
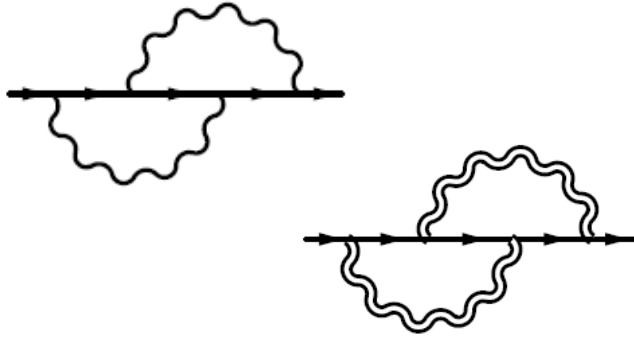
Second order exchange:

- In GW, vertex in self-energy

- No simple "physical" interpretation (as for exchange)

- Important to remove self-interaction

Particle-Hole ladder diagram:

- Electrostatic interaction between electrons and holes

- Excitonic effects

- Vertex corrections in W

- Important to remove self-screening

FAZIT

GW is an approximate method:
- Vertex in W: Neglect of e-h interaction.

- Vertex in Σ: Not self-interaction free for localized electrons
 In principle this is solvable, but very time consuming.
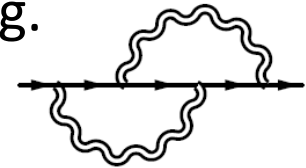
The best practical approaches right now:

Use G_0W_0 or GW_0 or possibly sc-QPGW_0 on top of
PBE, if PBE yields reasonable screening.

Possibly try G_0W_0 on top of HSE, if PBE is not reasonable, slightly
too large band gaps because RPA screening on top of HSE is not
great.

Strongly localized states might be wrong (too high) !

The GW potentials: *_GW POTCAR files
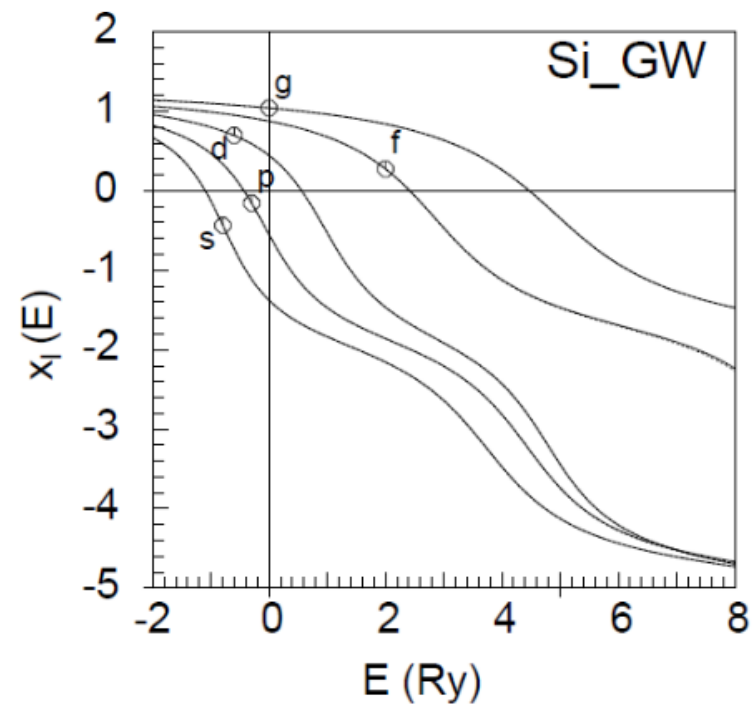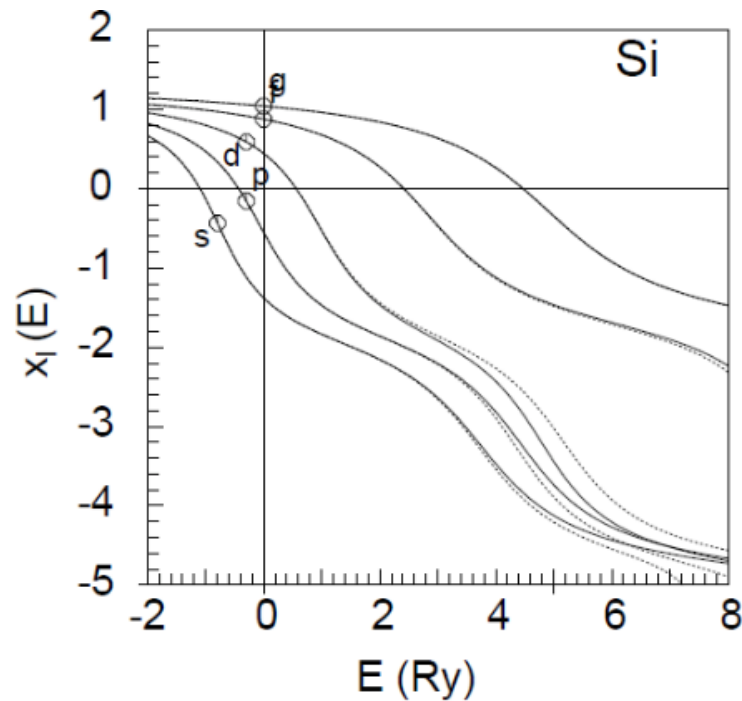
$\Delta(PAW)_{(VASP)} = 0.4$ meV/atom

H																	He
0,0																	0,0
Li	Be											B	C	N	O	F	Ne
0,1	0,5											0,2	0,2	0,7	0,1	0,1	0,1
Na	Mg											Al	Si	P	S	Cl	Ar
0,4	0,0											0,3	0,1	0,0	0,2	0,0	0,1
K	Ca	Sc	Ti	V	Cr	Mn	Fe	Co	Ni	Cu	Zn	Ga	Ge	As	Se	Br	Kr
0,1	0,4	0,3	0,3	0,1	0,8	0,1	0,1	0,2	0,8	0,5	0,6	0,8	0,7	0,8	0,4	0,2	0,1
Rb	Sr	Y	Zr	Nb	Mo	Tc	Ru	Rh	Pd	Ag	Cd	In	Sn	Sb	Te	I	Xe
0,1	0,2	0,5	0,4	0,2	0,9	0,1	0,2	0,3	0,4	0,3	2,5	0,2	0,2	0,5	0,9	0,9	0,1
Cs	Ba	Lu	Hf	Ta	W	Re	Os	Ir	Pt	Au	Hg	Tl	Pb	Bi	Po	At	Rn
0,1	0,3	3,5	1,7	0,8	1,2	0,9	0,5	0,8	0,3	0,1	1,0	0,2	0,1	0,5	0,6		0,0

RPA total energies (ACFDT)

The "RPA" total energy is given by:

$$E[n] = T_{KS}[\{\psi_i\}] + E_H[n] + E_X[\{\psi_i\}] + E_{\mathrm{ion-el}}[n] + E_c$$

with the RPA correlation

$$E_c = \sum_{\mathbf{q}} \int_0^\infty \frac{d\omega}{2\pi} \mathrm{Tr}\{\ln[1 - \chi_0(\mathbf{q}, i\omega)\nu] + \chi_0(\mathbf{q}, i\omega)\nu\}$$
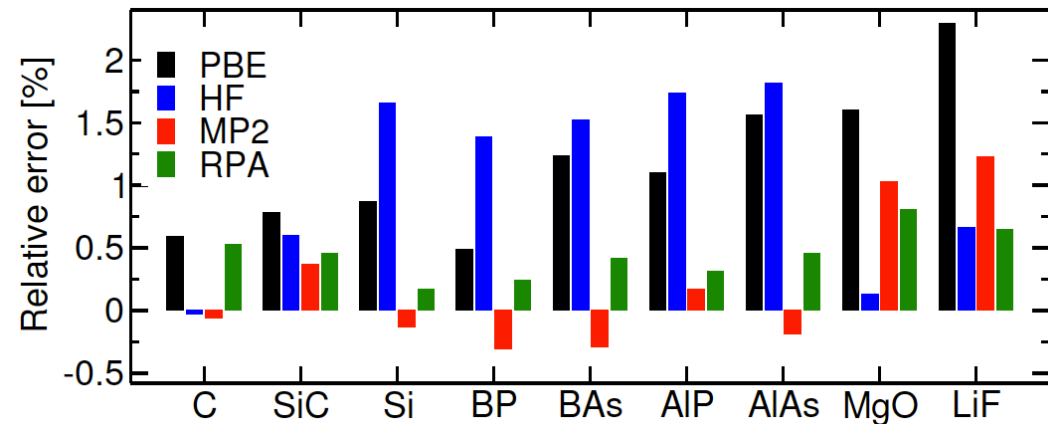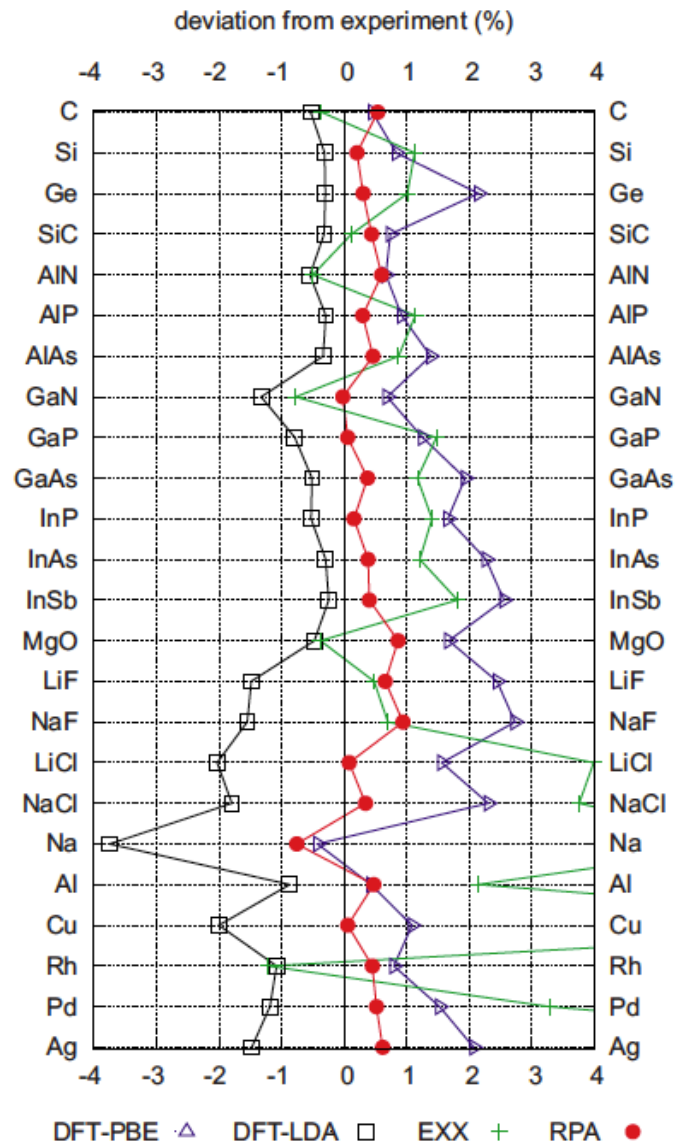
The main effort is (again) computing the IP polarizability:

$$\chi_{\mathbf{G},\mathbf{G}'}^0(\mathbf{q}, \omega) = \frac{1}{\Omega} \sum_{nn'\mathbf{k}} 2w_{\mathbf{k}}(f_{n'\mathbf{k}+\mathbf{q}} - f_{n'\mathbf{k}})$$

$$\times \frac{\langle\psi_{n'\mathbf{k}+\mathbf{q}}|e^{i(\mathbf{q}+\mathbf{G})\mathbf{r}}|\psi_{n\mathbf{k}}\rangle\langle\psi_{n\mathbf{k}}|e^{-i(\mathbf{q}+\mathbf{G}')\mathbf{r}'}|\psi_{n'\mathbf{k}+\mathbf{q}}\rangle}{\epsilon_{n'\mathbf{k}+\mathbf{q}} - \epsilon_{n\mathbf{k}} - \omega - i\eta}$$

Expensive: computing the IP-polarizability scales as N^4

RPA: lattice constants

J. Harl et al., PRB 81, 115126 (2010)
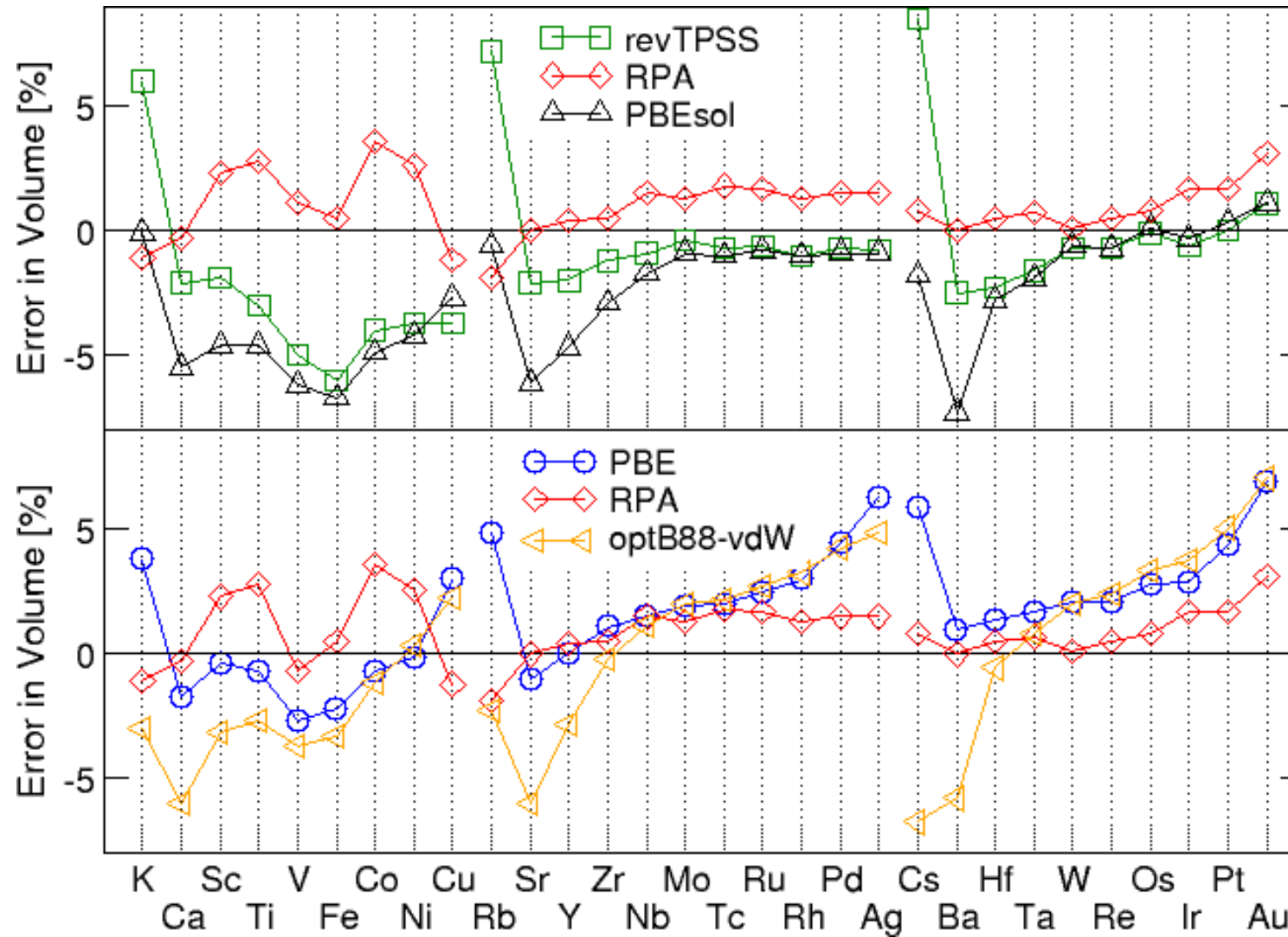

Deviations w.r.t. experiment
(corrected for zero-point vibrations)

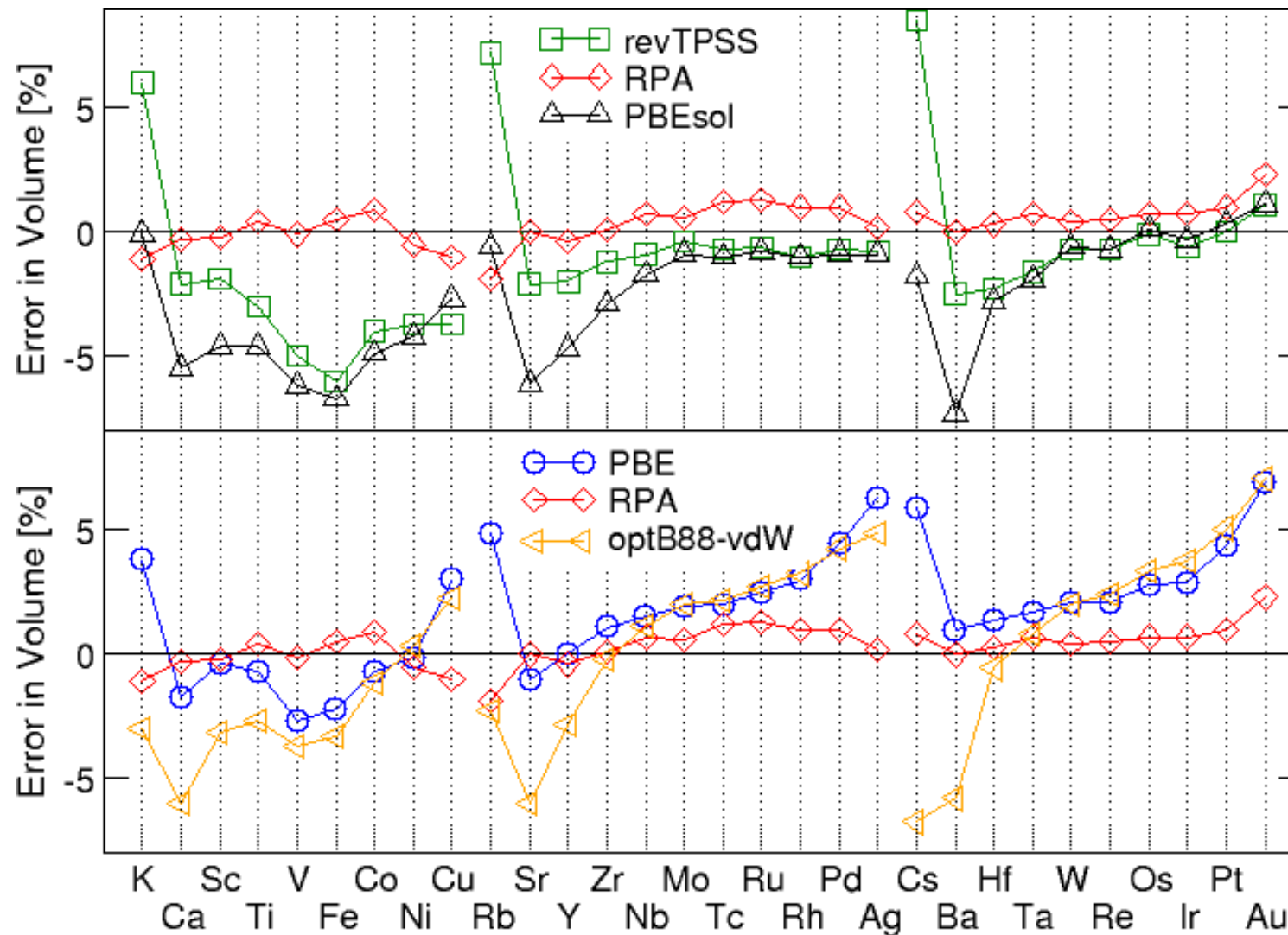|	MRE	MARE
PBE	1.2	1.2
HF	1.1	1.1
MP2	0.2	0.4
RPA	0.5	0.4

(in %)

RPA: TM lattice constants

Schimka, et al., Phys. Rev. B 87, 214102 (2013).
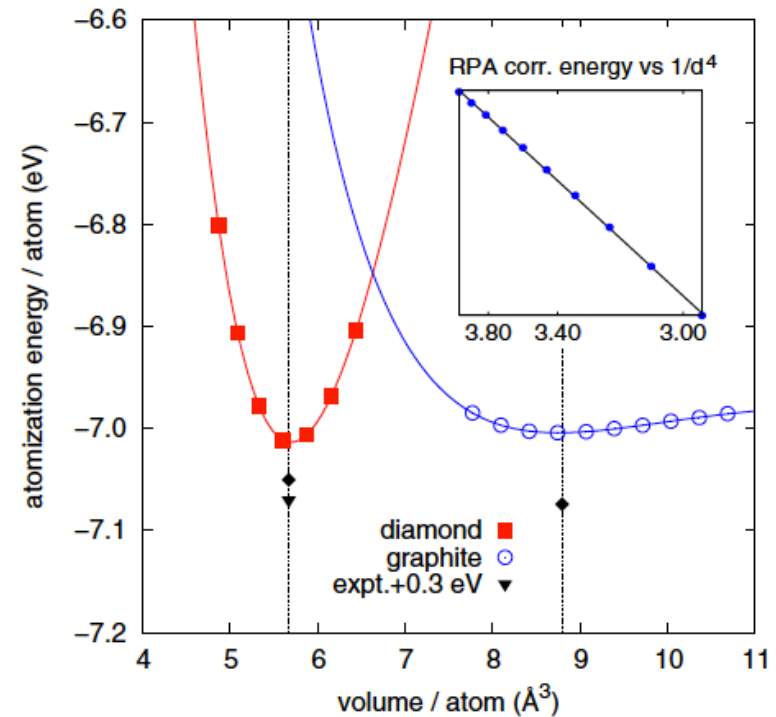
RPA: TM lattice constants (NC potentials)

NC-potentials: Klimeš, *et al.*, PRB 90, 075125 (2014).

RPA: atomization energies

J. Harl et al., PRB 81, 115126 (2010)

percent of exp. atomization energy

PBE ▨ EXX ▨ ACFD-RPA ▬

RPA corr. energy vs $1/d^4$

diamond ■
graphite ○
expt.+0.3 eV ▼
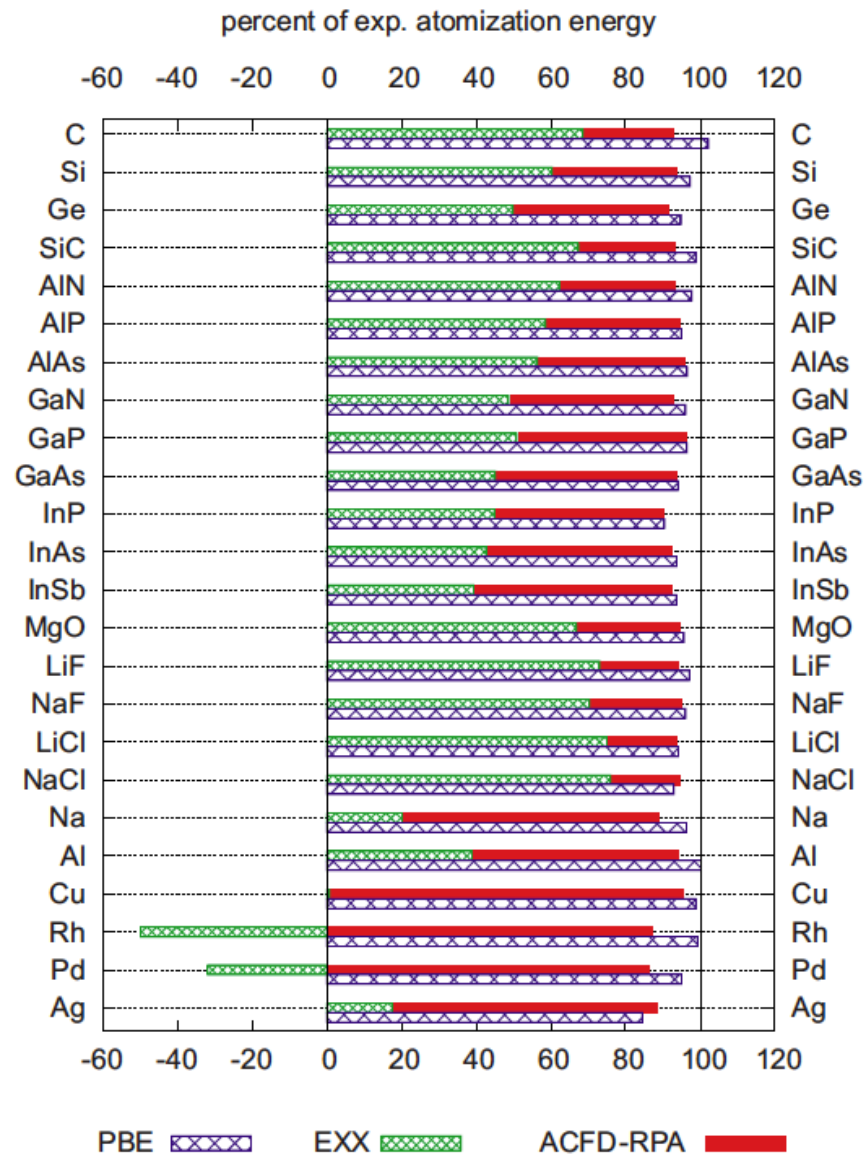
	Atomisation energies	
	MAE (eV)	MARE (%)
HF	1.65	
MP2	0.27	
PBE	0.17	5
LDA	0.74	18
RPA	0.30	7

Graphite vs. Diamond
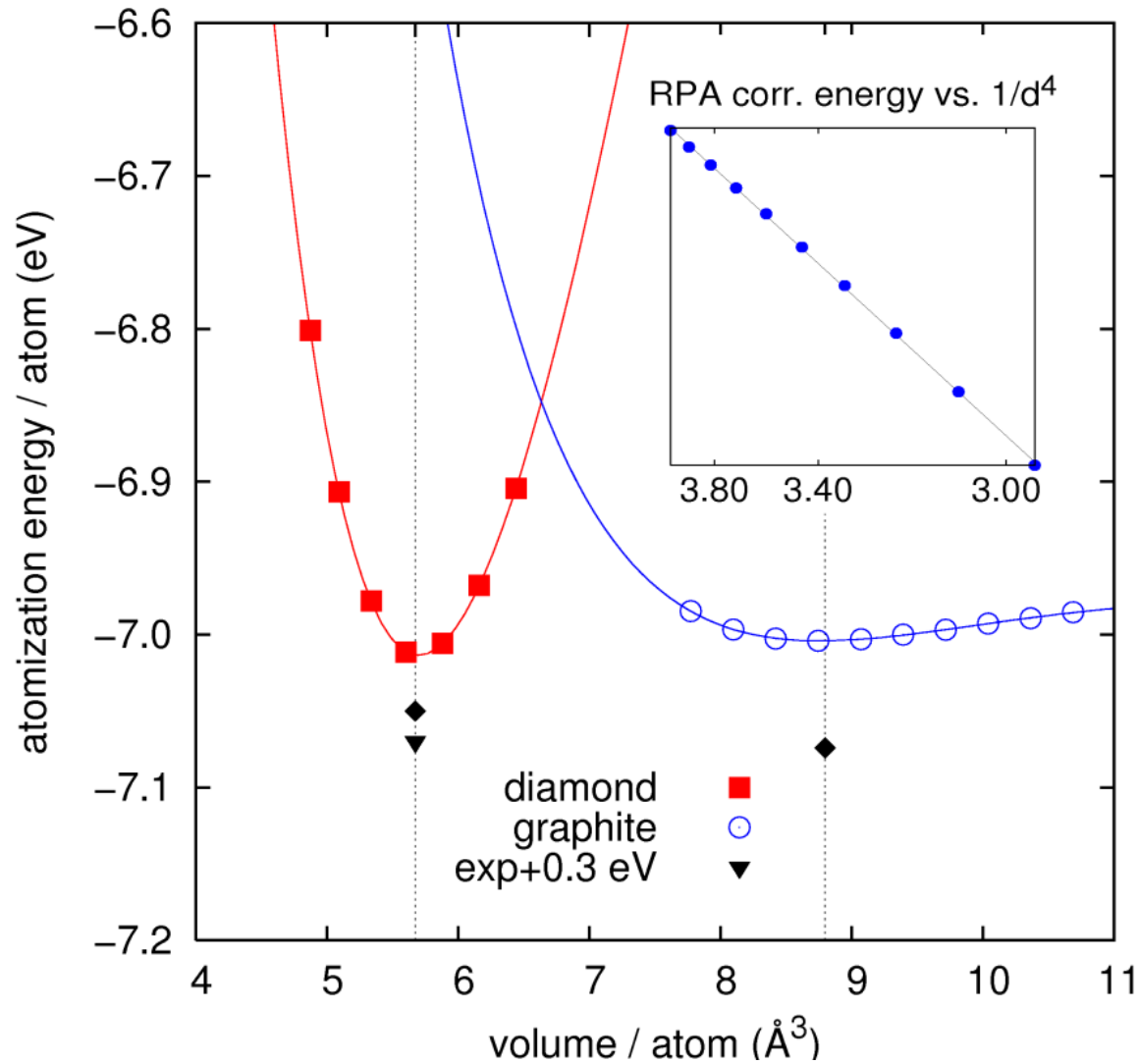
1/d⁴ behavior at short distances

	QMC (Galli)	RPA	EXP
d(Å)	3.426	3.34	3.34
C_{33}		36	36-40
E(meV)	56	48	43-50

J. Harl, G. Kresse,
PRL 103, 056401 (2009).
S. Lebeque, et al.,
PRL 105, 196401 (2010).

RPA: noble gas solids

J. Harl and G. Kresse, PRB 77, 045136 (2008)
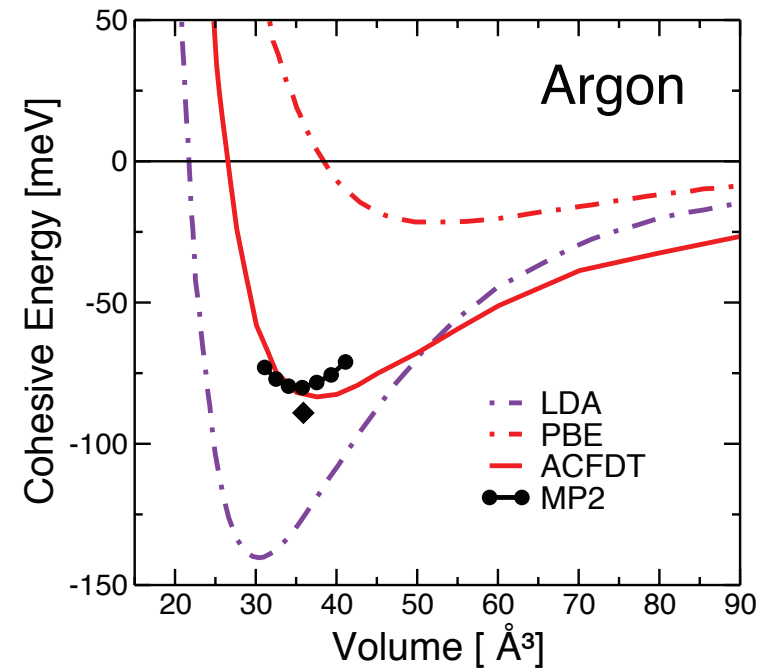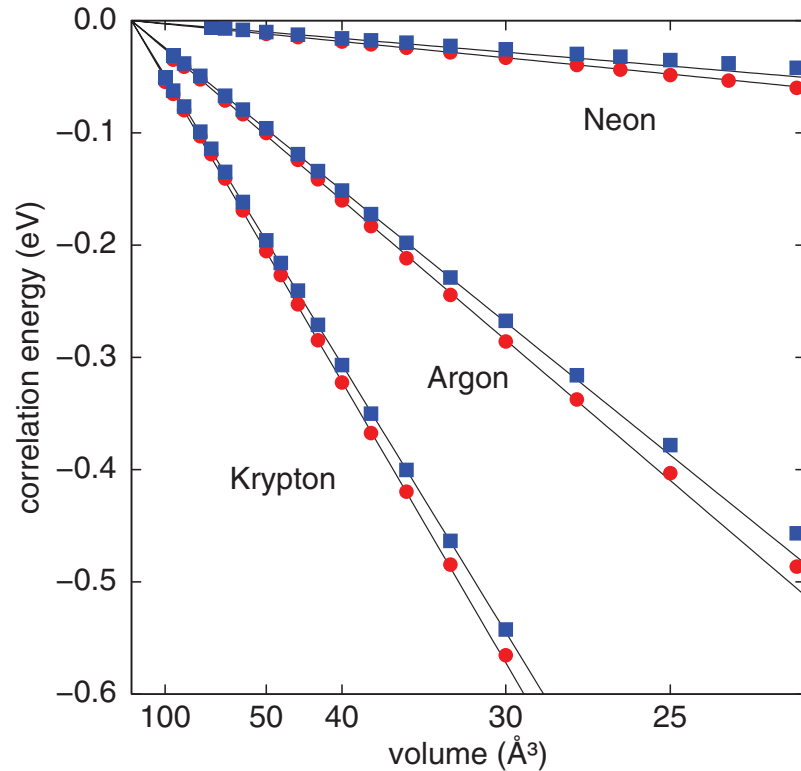
C_6 coefficients

	RPA(LDA)	RPA(PBE)	Exp.
Ne	62	53	47
Ar	512	484	455
Kr	1030	980	895

RPA: heats of formation
J. Harl and G. Kresse, PRL 103, 056401 (2009)

Heats of formation w.r.t. normal state at ambient conditions (in kJ/mol)

Example: Mg(bulk metal) + $H_2 \rightarrow MgH_2$

	PBE	Hartree-Fock	RPA	EXP
LiF	570	664	609	621
NaF	522	607	567	576
NaCl	355	433	405	413
MgO	516	587	577	603
MgH_2	52	113	72	78
AlN	262	350	291	321
SiC	51	69	64	69

RPA: heats of formation
J. Harl and G. Kresse, PRL 103, 056401 (2009)

TABLE I. Heats of formation at $T = 0$ K in kJ/mol (per formula unit) with respect to the elemental phases in their normal state under ambient conditions. Experimental values are collected in Ref. [33], if not otherwise stated, and have been corrected for zero-point vibrations (ZPV) (experimental values without corrections are in parentheses). The ZPV have been evaluated using harmonic *ab initio* phonon calculations.

Solid	PBE	LDA	EXX	RPA	Expt.
LiF[a]	570	613	664	609	619 (614)
NaF	522	558	607	567	577 (573)
NaCl	355	381	433	405	413 (411)
MgO[a]	516	595	587	577	604 (597)
MgH$_2$[a]	52	89	113	72	78 (68)
AlN	262	327	350	291	321 (313[b])
SiC	51	54	69	64	69 (72)

[a]bcc Li, hcp Mg, and rutile MgH$_2$ were considered in their experimental geometries, whereas for the other materials the theoretical minimum energy geometries were used.
[b]Ref. [34].

RPA: CO @ Pt(111) and Rh(111)
Schimka et al., Nature Materials 9, 741 (2010)

Top

Fcc
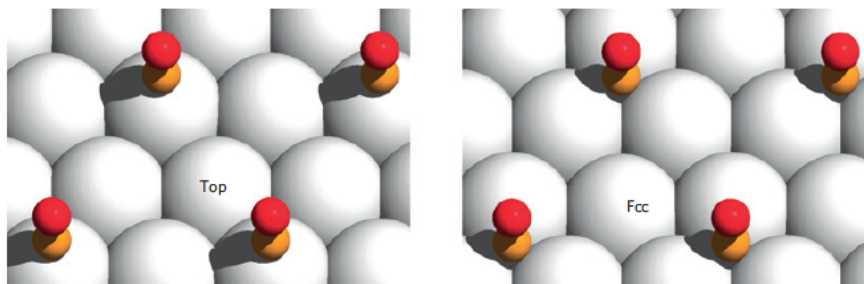
RPA:

- increases surface energy and
- decreases adsorption energy

FIG. 1: **Atop CO adsorption and surface energies for Pt(111) and Rh(111).** (a) Considered CO adsorption geometries for a (2×2) surface cell. Semi-local functionals predict CO to adsorb in the fcc hollow site coordinated to three metal atoms on Pt and Rh, whereas experiments unequivocally show adsorption atop a metal atom. (b) Atop adsorption energies versus surface energies for Pt(111) and Rh(111). Various semi-local functionals were used: AM05[10], PBEsol[11], PBE[8], rPBE[12] and BLYP[13], in order of increasing gradient corrections. Furthermore the hybrid functional HSE[18] based on the PBE functional was used.
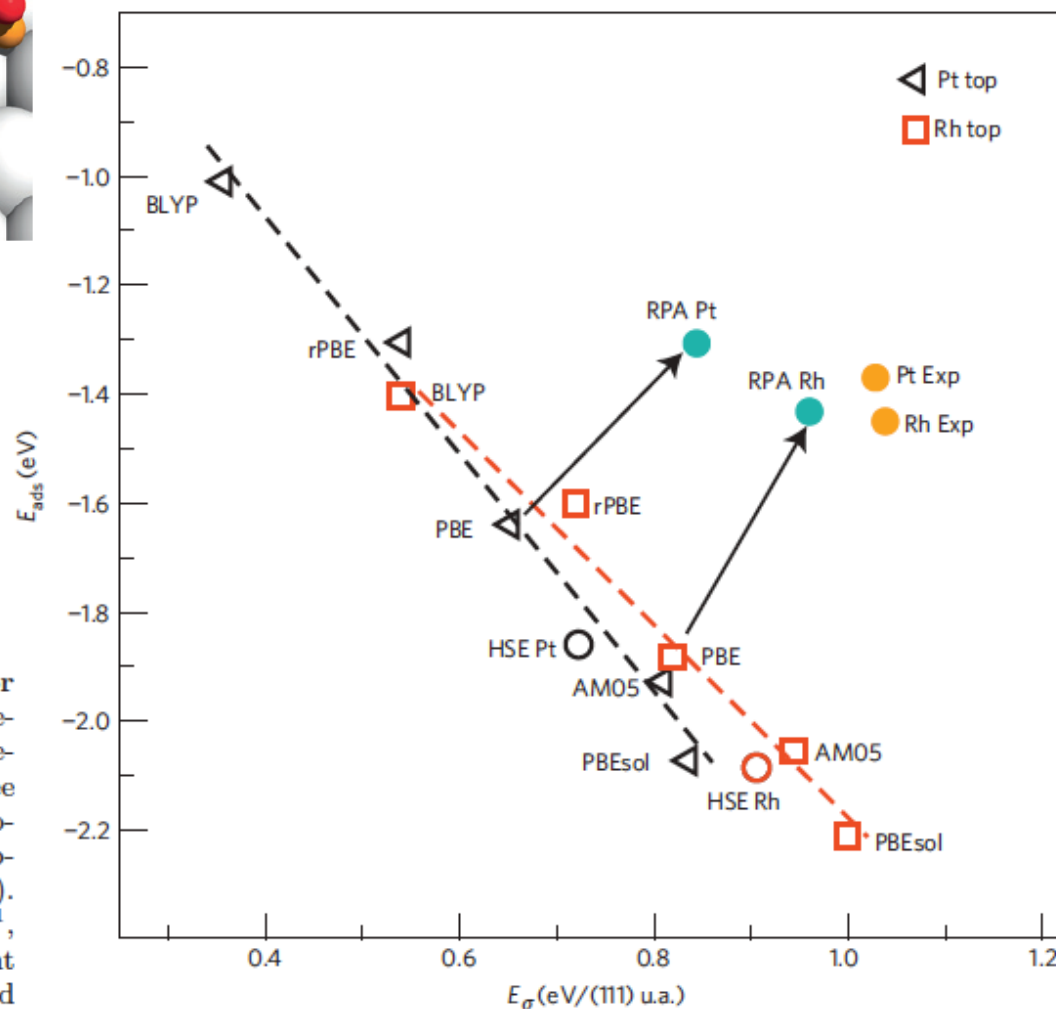
RPA:

- Right sight preference

- Good adsorption energies
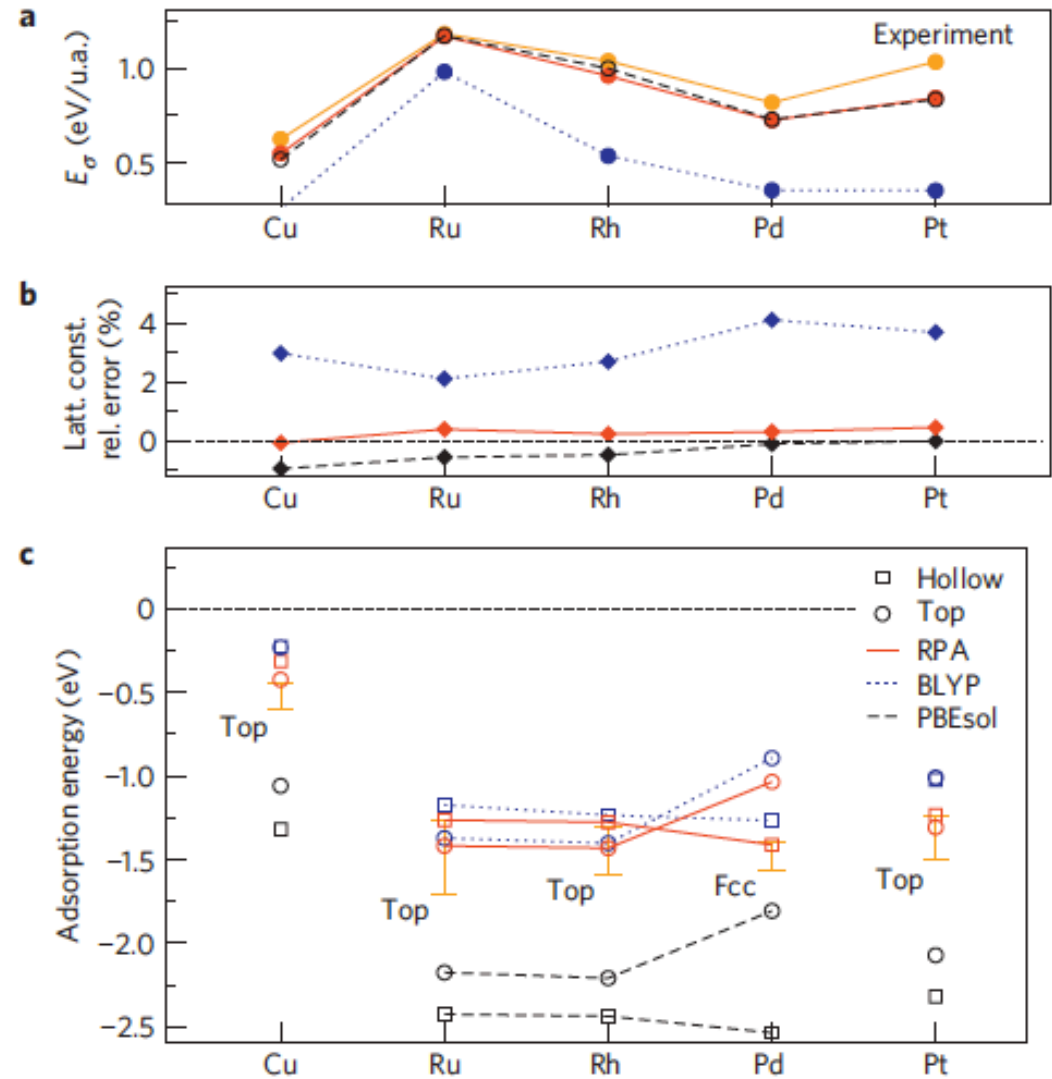
- Excellent lattice constants

- Good surface energies

Figure 3 | Surface energies, lattice constants and adsorption energies.
a, Fcc(111) surface energies (E_σ) for PBEsol, BLYP and RPA. Experimental surface energies are deduced from liquid-metal data[24,25]. **b**, Lattice constants for PBEsol, RPA and BLYP. **c**, Adsorption energies for the atop and hollow sites of CO on Cu, late 4d metals and Pt for PBEsol, RPA and BLYP. Experimental data with error bars are from ref. 26. The error bars correspond to the spread of the experimental results.

Schimka et al., Nature Materials 9, 741 (2010)

- DFT does well for the metallic surface, but not for the CO: $2\pi^*$ (LUMO) too close to the Fermi level.

- HSE does well for the CO, but not for the surface: d-metal bandwith too large.

- GW gives a good description of both the metallic surface as well as of the CO $2\pi^*$ (LUMO). The CO 5σ and 1π are slightly underbound.

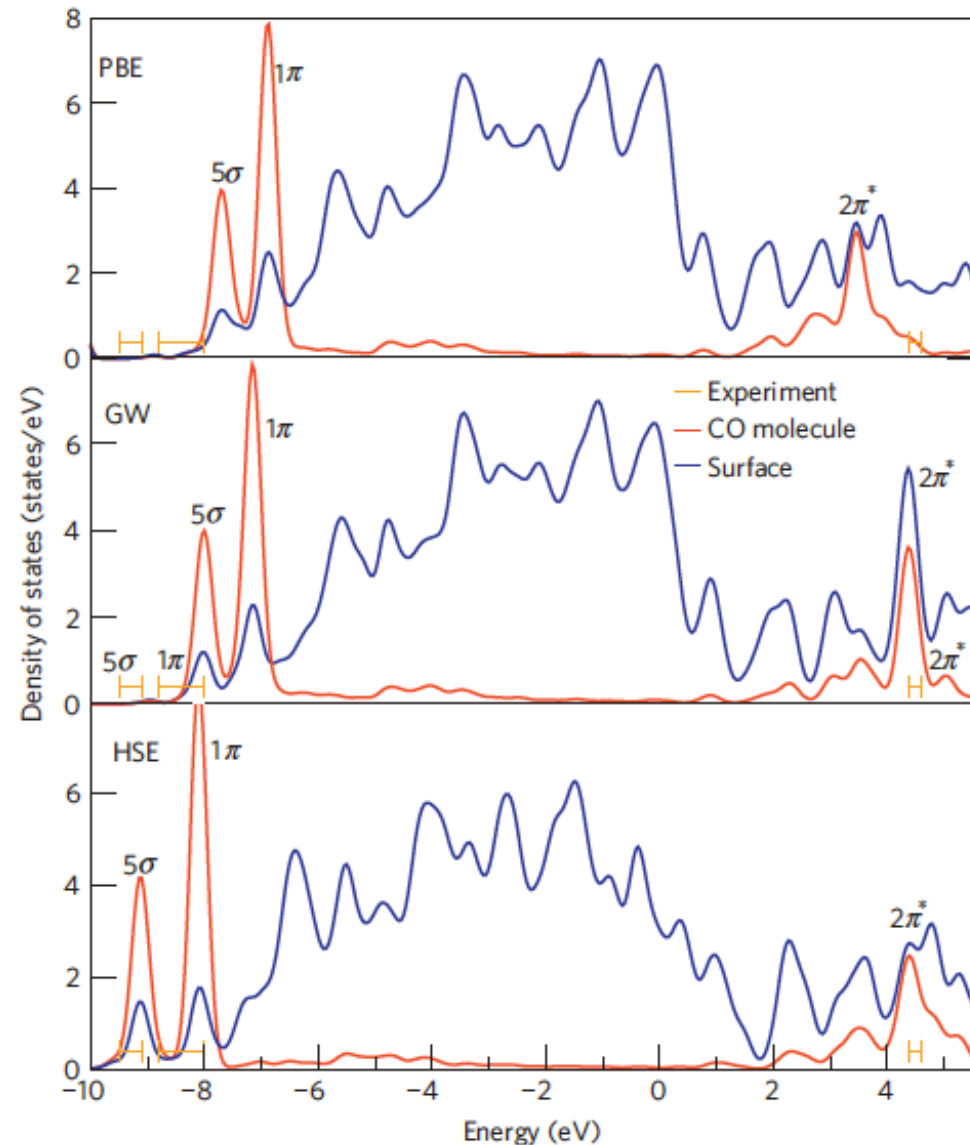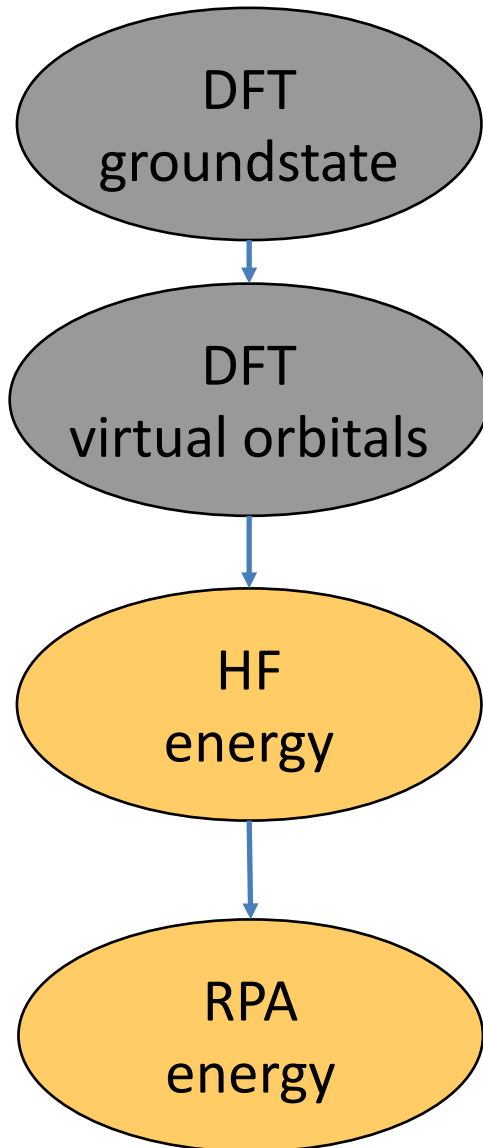Schimka et al., Nature Materials 9, 741 (2010)

Figure 2 | Electronic DOS for CO adsorbed atop a Pt atom on Pt(111). The DOS is evaluated using DFT (PBE), the RPA (GW) and a hybrid functional (HSE). Experimental photoemission data for the $2\pi^*$ state are from ref. 19, for the 5σ and 1π state from ref. 20.

RPA flow chart

As always: test, test, test, …

- **k**-point convergence is more difficult to attain
  than for DFT, in particular for metals.

    J. Harl, G. Kresse, PRB 81, 115126 (2010).

- ENCUTGW controls basis set for response functions.

- Increase ENCUT by about 25-30 % and recalculate everything
  (note NBANDS needs to be increased as well).

- Number of frequency points NOMEGA,…

FAZIT

- Well-balanced total energy expression that captures all types of bonding (equally) well, i.e., metallic, covalent, ionic, and *van-der-Waals*.

- Chemical accuracy? Unfortunately no .. but a definite improvement over hybrid functionals and DFT.

Cubic-scaling RPA

M. Kaltak, J. Klimes, and G. Kresse, PRB 90, 054115 (2014)

Evaluate the Green's function in "imaginary" time:

$$G(\mathbf{r}, \mathbf{r}', i\tau) = \sum_n \psi_n(\mathbf{r})\psi_n^*(\mathbf{r}')e^{-\epsilon_n \tau}$$

and the polarizability as:

$$\chi^0(\mathbf{r}, \mathbf{r}', i\tau) = -G(\mathbf{r}, \mathbf{r}', i\tau)G(\mathbf{r}', \mathbf{r}, -i\tau)$$

Followed by a cosine-transform:

$$\chi^0(\mathbf{r}, \mathbf{r}', i\tau) \xrightarrow{CT} \chi^0(\mathbf{r}, \mathbf{r}', i\omega)$$

Now the worst scaling step is

$$E_c = \int_0^\infty \frac{d\omega}{2\pi} \mathrm{Tr}\{\ln[1 - \chi^0(i\omega)v] + \chi^0(i\omega)v\}$$

which scales as N^3 due to the diagonalization involved in evaluating the "ln"

But storing G and χ is expensive! → we need small sets of cleverly chosen "τ" and "ω"

[see Kaltak et al., JCTC 10, 2498 (2014)]

Scaling

New RPA code (coming soon):

- Scales linearly in the number of k-points (as DFT), instead of quadratically as for conventional RPA and hybrid functionals

- Scales cubically in system size (as DFT).

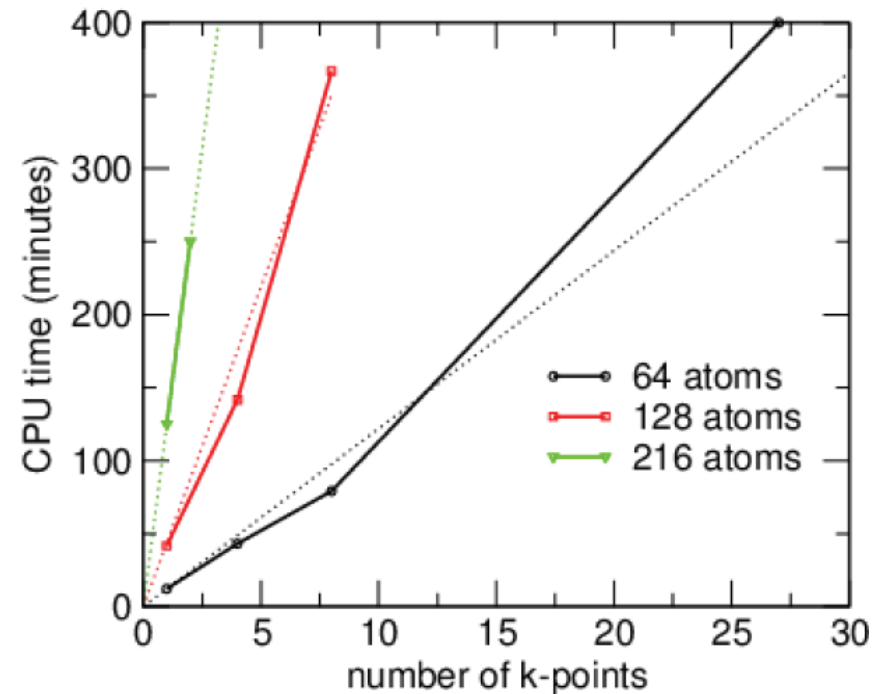Prefactors are much larger than in DFT, but calculations for 200 atoms take less than 1 hour (128 cores)

TABLE I. Timings in minutes for an RPA calculation for different bulk Si bcc cells. The calculations are done for the Γ point only and the number of cores is increased with system size. Since one of the computational steps scales only quadratically with system size, the total scaling is better than cubic.

Atoms	Cores	Time	Time$\times$cores/atoms$^3 \times 10^3$
54	32	14.3	2.91
128	64	83.2	2.54
250	128	299.9	2.45

Defect formation energies in Si

	PBE	HSE	HSE(+vdW)	QMC	RPA
Dumbbell X	3.56	4.43	4.41	4.4(1)	4.28
Hollow H	3.62	4.49	4.40	4.7(1)	4.44
Tetragonal T	3.79	4.74	4.51	5.1(1)	4.93
Vacancy	3.65	4.19	4.38		4.40

X   H

T   V
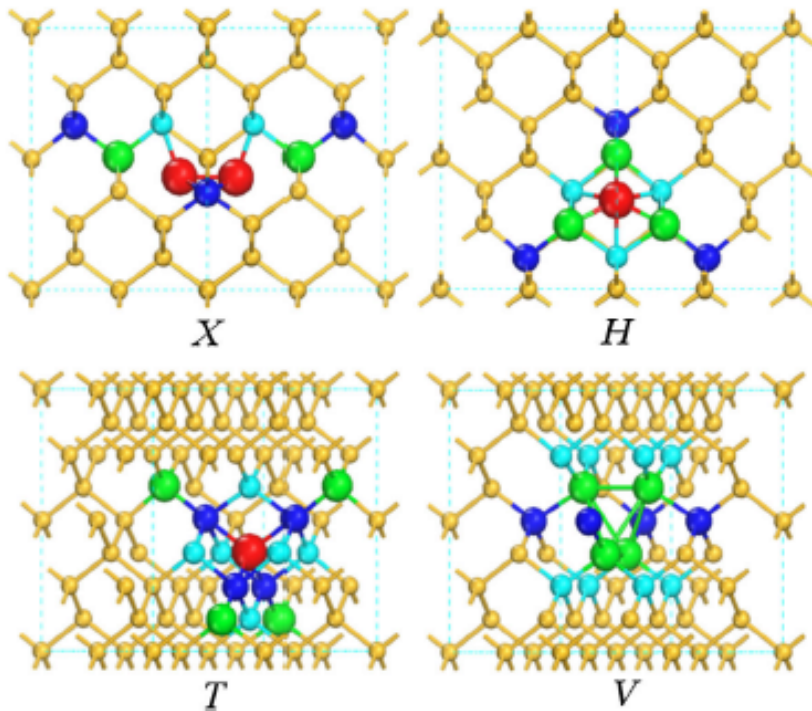
pictures and HSE+vdW:
Gao, Tkatchenko, PRL 111, 45501

QMC:
Parker, Wilkins, Hennig,
Phys. Status Solidi B 248, 267 (2011).

Cubic-Scaling GW

$$G_0(i\tau) \xrightarrow{\;\chi=-GG\;} \chi(i\tau) \xrightarrow{\;FT\;} \chi(i\omega)$$

$$W = \frac{V}{1-\chi V}$$

$$\Sigma(i\tau) \xleftarrow{\;\Sigma=GW\;} W(i\tau) \xleftarrow{\;FT\;} W(i\omega)$$

$$\Sigma(i\omega) \xrightarrow{\quad G=\dfrac{1}{G_0^{-1}-\Sigma}\quad} G(i\omega)$$

The End

Thank you!